Journal for ImmunoTherapy of Cancer

Intratumoral BO-112 in combination with radiotherapy synergizes to achieve CD8 T-cell-mediated local tumor control

Maria E Rodriguez-Ruiz ,[1,2,3,4] Irantzu Serrano-Mendioroz,[1] Eneko Garate-Soraluze,[1] Paloma Sánchez-Mateos,[5] Celia Barrio-Alonso ,[5] Inmaculada Rodríguez López,[1,2] Victor Diaz Pascual,[6] Leire Arbea Moreno,[3] Maite Alvarez ,[1] Miguel F Sanmamed,[1,2,3,4] Jose Luis Perez-Gracia,[2,3,4] Helena Escuin-Ordinas,[7] Marisol Quintero,[7] Ignacio Melero [1,2,3,4]

To cite: Rodriguez-Ruiz ME, Serrano-Mendioroz I, Garate-Soraluze E, *et al*. Intratumoral BO-112 in combination with radiotherapy synergizes to achieve CD8 T-cell-mediated local tumor control. *Journal for ImmunoTherapy of Cancer* 2023;**11**:e005011. doi:10.1136/jitc-2022-005011

► Additional supplemental material is published online only. To view, please visit the journal online (http://dx.doi.org/10.1136/jitc-2022-005011).

IS-M and EG-S contributed equally.

Accepted 26 September 2022

For numbered affiliations see end of article.

Correspondence to
Dr Ignacio Melero;
imelero@unav.es

ABSTRACT

Background Radioimmunotherapy combines irradiation of tumor lesions with immunotherapy to achieve local and abscopal control of cancer. Most immunotherapy agents are given systemically, but strategies for delivering immunotherapy locally are under clinical scrutiny to maximize efficacy and avoid toxicity. Local immunotherapy, by injecting various pathogen-associated molecular patterns, has shown efficacy both preclinically and clinically. BO-112 is a viral mimetic based on nanoplexed double-stranded RNA (poly I:C) which exerts immune-mediated antitumor effects in mice and humans on intratumoral delivery. BO-112 and focal irradiation were used to make the proof-of-concept for local immunotherapy plus radiation therapy combinations.

Methods Murine transplantable tumor cell lines (TS/A, MC38 and B16-OVA) were used to show increased immunogenic features under irradiation, as well as in bilateral tumor models in which only one of the lesions was irradiated or/and injected with BO-112. Flow cytometry and multiplex tissue immunofluorescence were used to determine the effects on antitumor immunity. Depletions of immune cell populations and knockout mice for the IFNAR and BATF-3 genes were used to delineate the immune system requirements for efficacy.

Results In cultures of TS/A breast cancer cells, the combination of irradiation and BO-112 showed more prominent features of immunogenic tumor cell death in terms of calreticulin exposure. Injection of BO-112 into the tumor lesion receiving radiation achieved excellent control of the treated tumor and modest delays in contralateral tumor progression. Local effects were associated with more prominent infiltrates of antitumor cytotoxic tumor lymphocytes (CTLs). Importantly, local irradiation plus BO-112 in one of the tumor lesions that enhanced the therapeutic effects of radiotherapy on distant irradiated lesions that were not injected with BO-112. Hence, this beneficial effect of local irradiation plus BO-112 on a tumor lesion enhanced the therapeutic response to radiotherapy on distant non-injected lesions.

Conclusion This study demonstrates that local BO-112 immunotherapy and focal irradiation may act in synergy to achieve local tumor control. Irradiation plus BO-112 in one of the tumor lesions enhanced the therapeutic effects on distant irradiated lesions that were not injected with BO-112, suggesting strategies to treat oligometastatic patients with lesions susceptible to radiotherapy and with at least one tumor accessible for repeated BO-112 intratumoral injections.

WHAT IS ALREADY KNOWN ON THIS TOPIC

⇒ Radiotherapy and immunotherapy approaches with checkpoint inhibitors can be combined to synergistically attain better tumor control in preclinical models, both on lesions receiving radiation and also outside the irradiation beam. Radiotherapy is being combined with immunotherapy in clinical trials. Intratumoral immunotherapy with the double-stranded RNA analog BO-112 as a viral mimetic has been tested in clinical trials showing safety and clinical activity in combination with anti-PD-1 agents.

WHAT THIS STUDY ADDS

⇒ This study preclinically opens the stage to the use of intratumoral immunotherapy agents in combination with radiotherapy. The combination with intratumoral BO-112 with radiotherapy resulted in excellent tumor control in three transplantable models, that was immune-mediated since therapeutic effects absolutely required CD8 T cells and conventional type-I dendritic cell-mediated crosspriming. However, only weak abscopal activity could be observed, even though distant effects could be markedly potentiated on combination with anti-PD-1 and anti-CTLA-4 mAbs.

HOW THIS STUDY MIGHT AFFECT RESEARCH, PRACTICE OR POLICY

⇒ These preclinical experiments warrant clinical testing of the proposed radioimmunotherapy combination strategy, which is being explored in a clinical trial for patients with oligometastatic NSCLC at our institution (Eudract 2021-006410-36). Moreover, these studies open the field of local/intratumoral immunotherapy interventions in combinations with radiotherapy.

INTRODUCTION

Marketing-approved immunotherapy strategies for cancer mostly rely on systemic

administration of immunotherapy agents. However, multiple preclinical mouse models have demonstrated that a variety of immunotherapy agents can be delivered locally to enhance antitumor immunity both in a local and systemic fashion.[1 2] Most of these agents are viral vectors or viral mimetics that raise the immunogenicity of tumor lesions seeking to turn them into in situ vaccines.[3] In the clinical setting, recombinant viral vectors,[3] STING agonists,[2 4] CpG oligonucleotides[5 6] and double-stranded RNA analogs[7] have promising records of safety and activity on local delivery, especially against melanoma and when combined with PD-(L)1 checkpoint inhibitors.[8 9] To date, the only approved agent of this type is a recombinant herpes simplex virus 1 encoding granulocyte-macrophage colony stimulating factor GM-CSF (T-Vec) although in combination with pembrolizumab, it did not surpass the efficacy of systemic pembrolizumab administered as a single agent to melanoma patients.[10]

BO-112 is a nanoplexed poly I:C polymer that mimics viral dsRNA to activate TLR3, MDA-5 and PKR.[11 12] This compound is able to elicit therapeutic effects against transplantable mouse tumor models when given intratumorally.[13] The mode of action involves the activation of type I interferon system and conventional type-I dendritic cells (cDC1) that are able to cross-present tumor antigens. Combinations with checkpoint inhibitors enhance BO-112 efficacy against the directly injected tumor, but more importantly, against modeled metastases.[13] Recently, we have reported that intratumoral co-injection of BO-112 and a STING agonist were synergistic against distant non-injected tumor lesions.[14] Phase I clinical trials with intratumoral BO-112 have shown excellent tolerability and evidence for activity in combination with nivolumab or pembrolizumab in PD-1 refractory patients,[8] especially in cases of melanoma.[9]

Radiotherapy (RT) also achieves its efficacy against cancer by acting locally. Ionizing radiation causes tumor cell death and some proinflammatory changes that can enhance anti-tumor immunity.[15] Cell death as elicited by ionizing radiation was found to be immunogenic in mouse models.[16–19] RT is considered an inducer of the so-called 'immunogenic cell death' characterized by molecular features that result in tumor antigens being cross-presented by activated dendritic cells that elicit antigen-specific cytotoxic T lymphocytes.[20–23]

RT has been used in combination with anti-CTLA-4 and/or anti-PD(L)1 checkpoint inhibitors showing synergistic effects in mouse models.[24–28] Preliminary clinical evidence for a potentially synergistic interaction has been reported.[25 26 29] Most of the randomized clinical trials have shown that combination of SBRT (stereotactic body radiation therapy), in a single tumor lesion, and immunotherapy does not result in increases of OS (overall survival) or PFS (progression free survival). Contrary to the original expectations, the abscopal effect is a rare event even when combining immunotherapy with radiation.[15]

Local RT has been used in combination with intratumoral CpG oligonucleotides for transplantable models of lymphoma[30] and clinical trials have tested low-dose RT and injection of CpG oligonucleotides yielding preliminary evidence for activity in non-Hodgkin's lymphoma and cutaneous T-cell lymphoma patients.[29 31 32] In mice, topical tumor treatment with the TLR-7 agonist cream, imiquimod (Aldara) showed synergistic effects with external beam RT against transplantable mouse models of breast cancer.[33 34] More recently, a combination of the poly ICLC dsRNA analog, Hiltonol, has been safely used together with sFLT3L for intratumoral delivery of both agents in patients suffering non-Hodgkin's lymphoma together with low-dose RT which was concomitantly delivered to only one of the tumor lesions.[35] The strategy offered proof for objective clinical responses and enhancement of antitumor immune responses.[35] Abscopal or distant effects are observed in consonance with previous experiences of RT and intratumoral Hiltonol delivery.[36]

In this study, we analyzed the combination of BO-112 and RT for transplantable tumors and show that the combination offers its best results on the control of the directly irradiated lesions, in a manner mediated by CD8 antitumor immune responses.

MATERIAL AND METHODS

Mice

Six-week-old female C57Bl/6 and BALB/c mice were purchased from Harlan Laboratories (Barcelona, Spain). C57Bl/6 *Batf3*$^{tm1Kmm/J}$ (Batf3$^{-/-}$) were kindly provided by Dr Kenneth M Murphy (Washington University, St Louis, Missouri) and bred at the CIMA animal facility. C57Bl/6 IFN-α/β Ro/o (IFNAR KO) were kindly gifted by Dr Matthew Albert (Institut Pasteur, Paris). Mice were housed in Centro de Investigacion Medica Aplicada (CIMA, Pamplona, Spain). Experimental protocols were approved by the Ethics Committee of the University of Navarra (CEEA058-20) according to European Council Guidelines.

Cell lines

The murine melanoma B16-OVA and colon carcinoma MC38 cell line were purchased from the ATCC. Cells were cultured in RPMI 1640 (Gibco) containing 10% fetal bovine serum (FBS, Sigma-Aldrich), 2 mM glutamine (Gln, Gibco), 100 U/mL penicillin and 100 µg/mL streptomycin (100 U/mL), and 50 µM 2-mercaptoethanol (Gibco). The B16-OVA cell line was supplemented with 400 µg/mL Geneticin (Gibco). The TS/A mouse breast carcinoma cell line and its clones were kindly gifted by Dr Lorenzo Galuzzi (Weill Cornell Medical College, New York, New York, USA). All clones were cultured in DMEM (Gibco) containing 4.5 g/L glucose, 4 mM L-glutamine and 110 mg/L sodium pyruvate, supplemented with 100 mM HEPES buffer and 10% FBS (complete culture medium), 2 mM glutamine (Gln, Gibco), 100 U/mL penicillin and 100 µg/mL streptomycin (100 U/mL), and 50 µM 2-mercaptoethanol. Cell lines were routinely

tested every 2 months for mycoplasma contamination (MycoAlert Mycoplasma Detection Kit, Lonza).

Clonogenic assays

The in vitro loss of viability of cells after the treatment with ionizing radiation and exposure to BO-112 in mouse cell lines was assessed by clonogenic assays. B16-OVA and TS/A cell lines were seeded in 6-well plates with serially decreasing numbers: 50, 100, 200, 400, 800 or 1600. Culture medium was added to a final volume of 2 mL per well. The following day, BO-112 or 5% glucose was added to culture media at 0.4 µL/mL. One day later, plates were irradiated at 0 Gy, 1 Gy, 3 Gy or 5 Gy and culture medium was replaced. Plates were cultured in an incubator and left at 37°C and 5% CO_2 for 10–14 days. After fixation with ethanol, 70% colonies were stained and visualized with 0.1% crystal violet for 15 min.[37]

Cell death

Control and caspase3$^{-/-}$ TS/A clones were seeded in 6-well plates and treated with BO-112+/- a single irradiation fraction of either 8 Gy. Cells and supernatants were collected 24 and 48 hours later and apoptosis markers were studied. Cells were stained with the vital dye propidium iodide (PI) and fluorescent annexinV (AnnV) to analyze cell viability by flow cytometry. Immunogenic cell death markers were also analyzed in cell cultures by flow cytometry or in supernatants by ELISA. Cells were stained with anti-calreticulin (CRT) as the primary antibody and anti-rabbit IgG (FITC) as the secondary antibody to analyze surface presence of CRT by flow cytometry. Concentrations of IFN-β in culture supernatants were determined with the corresponding sandwich ELISA kits following the manufacturers' instructions (VeriKine-HSTM Mouse Interferon Beta Serum ELISA Kit from PBL Assay Science and IBL International ST51011, respectively). ATP concentrations were determined using the Via Light plus kit (Lonza) following the manufacturer's instructions.

Mouse models

To determine the abscopal effect 0.5×10^6 B16-OVA or MC38 cells were subcutaneously injected into the right flank while 0.25×10^6 cells were injected into the left flank of 8-week-old to 10-week-old female C57BL/6 mice on day 0. For TS/A cells, 0.2×10^6 cells were subcutaneously injected into the right flank, whereas 0.1×10^6 were injected into the left flank of 8-week-old to 10-week-old female BALB/C mice. Tumors were measured twice weekly with calipers and the volume calculated (length × width^2/2). When tumors reached a volume of 80–100 mm^3, mice were randomized into different experimental treatment groups.

In vivo experiments

To determine the abscopal effect, and depending on the mouse tumor model, 5×10^5 MC38, B16-OVA or 2×10^5 mouse mammary adenocarcinoma TS/A tumor cells were subcutaneously injected into the right flank of C57BL/6 (MC38 or B16-OVA) or BALB/c (TS/A) mice, whereas the left flank received a subcutaneous injection of 2.5×10^5 (MC38 or B16-OVA) or 1×10^5 (TS/A) tumor cells. When right tumors reached a tumor volume of 80–100 mm^3 and both tumors were palpable, mice were randomized into different treatment groups and, depending on the experiment, right tumors were injected intratumorally with 50 µg (2.5 mg/kg) of BO-112 (Highlight Therapeutics, Valencia, Spain), or 5% glucose, twice per week for 3 weeks (six doses in total). The last dose of BO-112 or vehicule was indicated with a dotted line in the schema of treatment. Intratumoral injection was administer with or without hypofractionated focal irradiation (8 Gy×3 fractions), to only one of the two tumors. RT was delivered with the Small Animal Radiation Research Platform (SARRP, from Xstrahl) on days 10, 11 and 12. In some experiments, irradiation was administered on days 12, 13 and 14. Tumors was monitored every 2–3 days and mice were sacrificed when tumor size reached 2000 mm^3. In some experiments, RT was combined with approved immune checkpoint blockade. PD-1 and CTLA-4 blockade therapy was provided by intraperitoneal injection of 100 µg of anti-PD-1 (clone RMP1-14, BioXcell) and anti-CTLA-4 (clone 9D9, BioXcell) on days 10, 13, 17, 20, 24 and 27 and on days 12, 15 and 18, respectively. Control mice received intraperitoneal injections of rat and mouse IgG, respectively. In some experiments, C57BL/6 mice deficient for BATF3, interferon-α/β receptor (IFNAR)1 or their wild-type counterparts were used. FTY720 (Enzo) or vehicle (PBS) was given intraperitoneally at 100 µg per dose from day 9 until the end of the experiment.

In vivo depletion of CD4 and CD8 T cells

Depletion of CD4 or CD8 T cells was achieved by intraperitoneal injection of anti-mouse CD4 (clone GK1.5) and CD8 β (clone 53–5.8.) monoclonal antibodies, produced and purified by affinity chromatography on protein-G from the corresponding hybridomas. Anti-mouse CD4 and anti-mouse CD8β monoclonal antibodies were administrated at days 9, 12, 16, 20, 23 and 27 at 100 ug per dose. During the experiment, blood samples were taken and analyzed by flow cytometry, showing that mice were completely depleted of the corresponding lymphocyte subset.

In vivo killing assays

Experiments were carried out in mice bearing B16-OVA tumor-bearing mice, following the instigation of RT (8 Gy/3fraction) plus intratumoral BO-112 (2.5 mg/Kg) at day 10 and 13. On day 19, half of the splenocytes from naive mice were pulsed with 10 µg/mL OVA257–264 peptide (SIINFEKL) and the other half with medium, followed by staining with 2.5 µM (high) or 0.25 µM (low) CFSE, respectively. Splenocytes were transferred intravenously (5×10^6 cells from each population) into the indicated mice groups. Twenty-four hours later, mice were sacrificed. Spleens were excised to analyze in vivo cytotoxicity using a CytoFLEX Flow cytometer (BD Biosciences). The percentage of specific lysis was calculated

using the formula ((100 − [(100 × (%CFSE ^{high} primed mice/%CFSE ^{low} primed mice)]/(%CFSE ^{high} naive mice/%CFSE ^{low} naive mice)). CytExpert software was used for data analysis.

Flow cytometry

To obtain unicellular cell suspensions, draining and non-draining lymph nodes were mechanically disrupted and passed through a 70 µm cell strainer (BD Falcon, BD Bioscience) by pressing with a plunger. Single-cell suspensions were treated with FcR-Block (anti-CD16/32 clone 2.4G2, BD Biosciences) in a PBS-based buffer containing 10% fetal calf serum to avoid unspecific staining. Tetramer staining was performed according to the manufacturer's protocol using an anti-mH-2Kb bound to the SIINFEKL antibody. Flow cytometry antibodies, tetramers, cell death staining and isotype control are listed in table 1. For intracellular FoxP3, granzyme B and Ki-67 staining, cells were fixed and permeabilized using the True-Nuclear Transcription Factor Buffer Set (BioLegend).

Samples were acquired in a CytoFLEX Flow cytometer (BD Biosciences) and CytoFLEX S Flow cytometer (Beckman Coulter) and CytExpert software was used for data analysis.

Multiplexed immunofluorescence

B16-OVA xenografts cryosections were fixed with cold acetone for 10 min, stained with different antibodies and analyzed by confocal microscopy. For immune phenotyping, samples were stained with CD8a-647 (BioLegend 100724, clone 53–6.7), CD4-FITC (BD Bioscience 553046, clone RM4-5), F4/80-647 (BioLegend 123122, clone BM8), MHCII-FITC (BD Bioscience 553623, clone 2G9), CLEC9A (Thermo Fisher PA5-47872) antibodies. All quantifications were performed in 3–5 20× fields. Imaging was performed using the glycerol ACS APO 20× NA0.60 immersion objectives of a confocal fluorescence microscope (SPE, Leica-Microsystems), and FIJI software was used for image quantification in all cases, as previously shown (JID22).

Statistical analysis

Statistical analyses were performed using Prism software (GraphPad Prism 6, La Jolla, California, USA). One-way analysis of variance (ANOVA) tests with Bonferroni post-test analysis, two-way ANOVA tests with Bonferroni post-test analysis and log-rank tests were used when appropriate to determine statistical significance. The Mantel-Cox test was used for survival analysis. Values of $p<0.05$ (*), $p<0.01$ (**) and $p<0.001$ (***) were considered significant.

Table 1 Antibodies for flow cytometry.

FC mAb and other stainings	Clone	
Anti-mCD4 BUV496	GK1.5	BD Bioscience
Anti-mCD8 BUV395	53–6.7	BD Bioscience
Anti-mCD25 BV421	PC61	BioLegend
Anti-mCD45 BV510	30-F11	BioLegend
Anti-mPD-L1 APC	10F.9G2	BioLegend
Anti-mPD-1 BV785	29F.1A12	BioLegend
Anti-mCD40 PerCP-eFluor 710	1C11	eBioscience
Anti-mCD137 Biot	17B5	BioLegend
Anti-mFoxP3 PECy7	3G3	Abcam
Anti-mGranzymeB FITC	NGZB	eBioscience
Anti-mki67 AF700	16A8	BioLegend
Anti-mH-2Kb bound to SIINFEKL Antibody	25-D1.16	Biologend
Anti-mCD45.2 P.Blue	104	BioLegend
Anti-mCD11b BUV395	M1/70	BD Bioscience
Anti-mCD11c PerCPCy5.5	N418	BioLegend
Anti-mF4/80 PECy7	BM8	BioLegend
Anti-mCD103 PE	.2E7	BioLegend
Anti-mLy6C FITC	HK1.4	BioLegend
Anti-mLy6G BV510	1A8	BioLegend
Anti-mXCR1 APC	ZET	BioLegend
Anti-mI-Ab Biot	KH74	BD Bioscience
Anti-Rat IgG2a FITC	RTK2758	BioLegend
Anti-mCD8a-AF647	53–6.7	BioLegend
Anti-mCD4-FITC	RM4-5	BD Bioscience
Anti-mF4/80-AF647	BM8	BioLegend
Anti-mMHCII-FITC	2G9	BD Bioscience
Anti-mCD31	2H8	Thermofisher
Anti-mCLEC9A		Thermofisher
Anti-mActive Caspase3		R&D
Anti-mCalreticulin antibody - ER Marker		Abcam
PromoFluor 840		Promocell
Anti-mAnnexin V FITC		BioLegend
IP		Pharmingen
Zombie-NIR		BioLegend

The table lists all antibodies used in this study, including clone and provider.

RESULTS

BO-112 plus RT induces immunogenic cell death in a fraction of malignant cells

Both RT and BO-112 have been shown to cause immunogenic cell death in cultured tumor cells.[13 19] We observed in cultured TS/A mouse breast cancer cells that irradiation and BO-112 synergized to reduce the fraction of viable cells in classic 14-day clonogenic assays (figure 1A). Next, we addressed whether death was mediated by classic caspase 3-dependent apoptosis and whether there were molecular features of apoptosis associated with immunogenic cell death in cultures set up as described in figure 1B. Propidium iodide (PI) and annexin V staining showed that cell death was indeed synergistically induced by the combination of BO-112

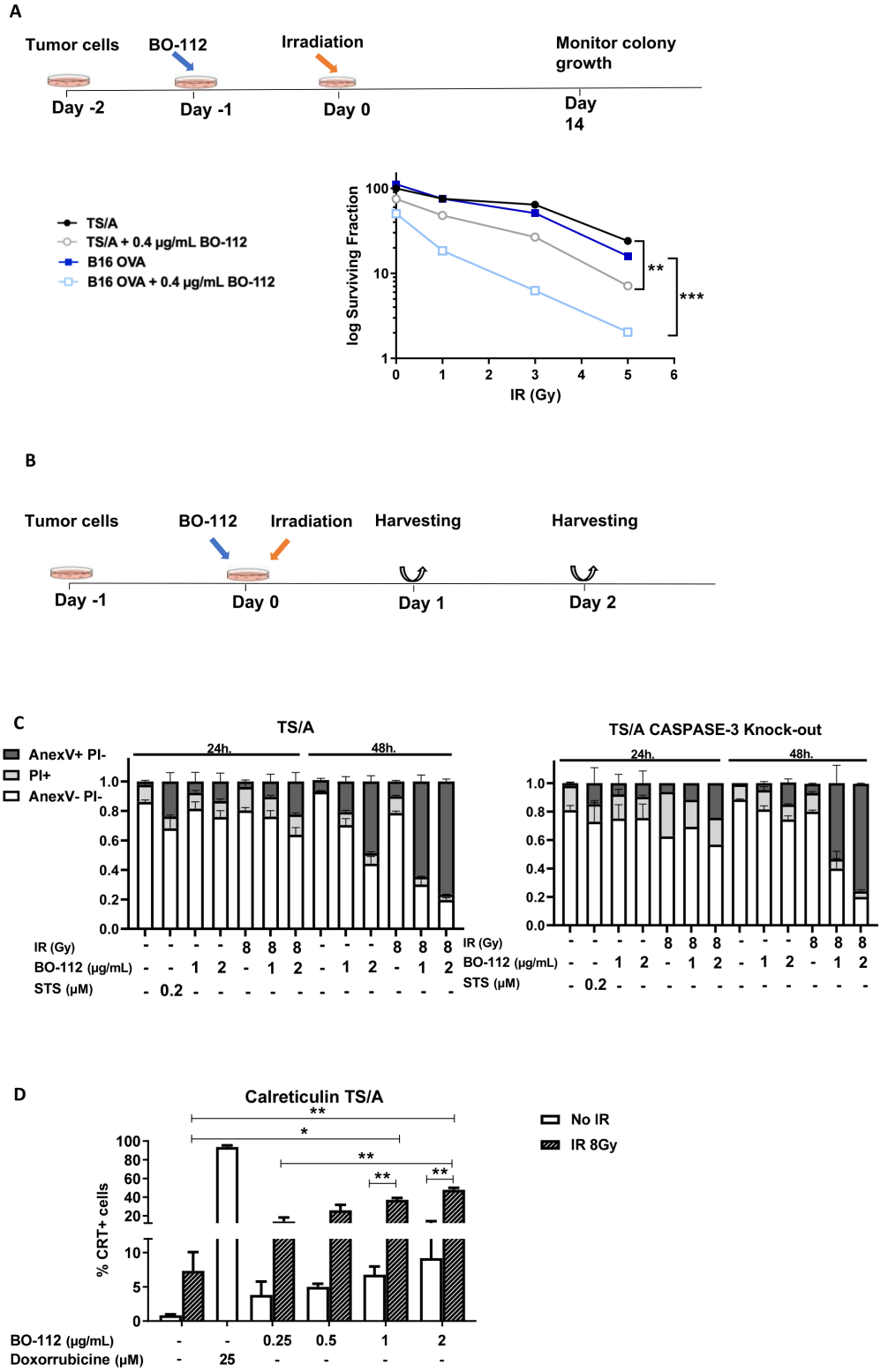

Figure 1 BO-112 in conjunction with irradiation induces immunogenic cell death in cultured cancer cell lines. (A) Scheme and results of clonogenic assays of cultures derived from the TS/A breast cancer cell line and B16-OVA cell line when treated with BO-112 and/or irradiation as indicated. The log fraction of surviving colonies with or without BO-112 treatment is represented for the graded doses of irradiation. Two independent experiments with triplicate wells were pooled and dots represent the mean. **p<0.01, ***p<0.001 (one-way ANOVA, as compared with untreated cells). (B and C) Scheme and results of 24-hour and 48-hour cultures of TS/A cells that were irradiated or/and cultured in the presence of BO-112 at the indicated concentrations. The fraction of cells stained with propidium iodide (PI) or annexin V was analyzed by flow cytometry at the end of such cultures. TS/A cells (left panel) and TS/A cells in which caspase 3 gene had been knocked down (right panel) were tested.[38] (D) Calreticulin surface staining of TS/A cells treated as in B. Results show means±SEM, n=2–3 independent experiments, *p < 0.05, **p<0.01.

and irradiation in a dose-dependent fashion (figure 1C). Interestingly, when using previously described caspase 3 knock-out TS/A cells,[38] the killing effect of BO-112, RT or the combination was preserved, indicating caspase 3 independence (figure 1C).

Calreticulin exposure on the outer leaf of the plasma membrane is an 'eat-me' signal that is associated to immunogenic cell death.[23] Analyzing the TS/A cultures at 48 hours showed that RT induced prominent calreticulin exposure and that BO-112 also induced it to some extent and enhanced the levels achieved by ionizing irradiation (figure 1D and online supplemental figure 1A). The synergistic effects of BO-112 and irradiation concur with signs of calreticulin-induced cell stress. This coincided with evidence for cell death and apoptosis but not pyroptosis (caspase 3 was not required). Indeed, our results are consistent with the Kroemer group's findings[39] concluding that, while cell stress is essential, it is not necessarily sufficient to produce immunogenic cell death. Therefore, cell stress and immunogenic cell death are two distinct but connected entities. ATP and IFN-β release to the milieu are considered important features of immunogenic cell death. We observed that exposure to BO-112 and to ionizing irradiation increased IFN-β and ATP concentrations in the TS/A culture supernatants, although the two stimuli did not cooperate to attain even higher concentrations (online supplemental figure 2A,B).

Intratumoral injection of BO-112 and RT has a synergistic effect controlling tumor growth in the treated lesion and delaying progression of distant untreated tumors

Experiments were carried out in three bilateral transplantable syngeneic mouse models developing subcutaneous tumors in opposite flanks. Tumors were implanted and mice were treated with RT or/and intratumoral BO-112 as indicated in figure 2A. In this experimental setting, RT or BO-112 alone only attained a minor efficacy against the directly treated MC38-derived tumors which had grown for 12 days before treatment onset and were well established. In contrast, the combination of BO-112 and RT completely controlled the directly treated tumors in most instances and even slightly delayed the progression of the contralateral tumor nodules (figure 2B,C). These results were recapitulated in TS/A bilateral tumors (figure 2D–F) and in the case of B16-OVA-derived

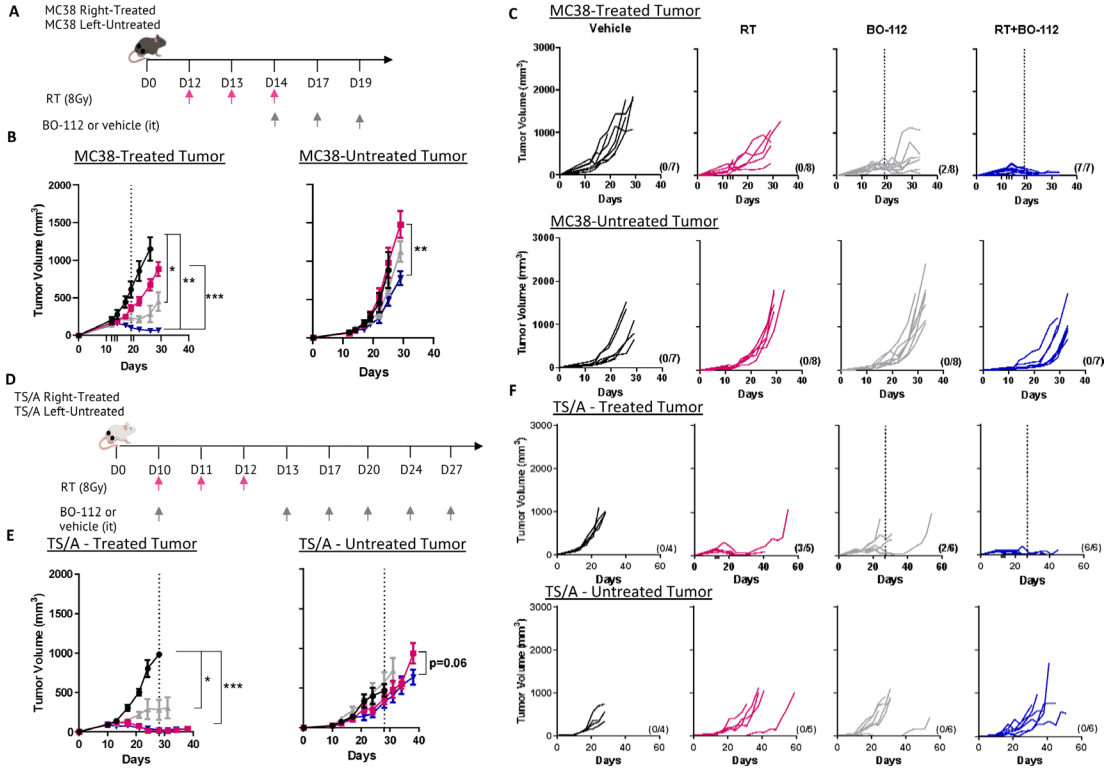

Figure 2 Local BO-112 synergizes with radiotherapy to control irradiated tumor lesions. (A) Scheme of 12-day tumor engraftment and subsequent treatments with hypofractionated radiotherapy and intratumoral injections of BO-112 in bilateral subcutaneous MC38-derived tumors whose size was monitored. Radiotherapy and BO-112 were given to the same tumor lesions. (B) Means±SEM and statistical comparisons among experimental groups *p<0.05, **p<0.01, ***p<0.001 (two-way ANOVA). (C) Individual tumor sizes in the treated and distant untreated tumors as indicated. The dotted line indicates the last intratumoral injection of BO-112. (D) The percentage of survival over time is shown for experiments in B. (E) Same schemes of treatment of bilateral TS/A-derived tumors treated as indicated with radiotherapy and/or intratumoral BO-112 at the irradiated tumor site. (F) Means±SEM and statistical comparisons among experimental groups *p<0.05, ***p<0.001 (two-way ANOVA). (G) Individual size of treated and untreated tumor lesions. (H) The percentage of survival until 50 days is shown for experiments in F.

bilateral tumors (online supplemental figure 3). Of note, dosimetry analyses of the distant tumors indicated virtual absence of irradiation doses received by such distant tumor sites (online supplemental figure 4).

Given the fact that immunotherapy is frequently tested in the clinic in the context of checkpoint inhibitor backbones,[40] we studied if the addition of anti-PD-1 or/and anti-CTLA-4 mAbs would strengthen the abscopal effect in the same models (online supplemental figure 5A).

We next tested if the quadruple combo treatment (anti-PD-1 mAbs+CTLA-4 mAbs+BO-112+RT) induced a clear enhancement of abscopal efficacy in mice carrying on bilateral TS/A-derived tumors (online supplemental figure 5B,C) and indeed it attained abscopal effects.

Requirements of CD8 T cells, conventional type 1 dendritic cells and the type I IFN system for the efficacy of BO-112 plus RT

To study the immune system requirements for the efficacy of intratumoral BO-112 plus RT in combination, we performed selective depletions of CD4 and CD8 T cells with specific monoclonal antibodies. As shown in figure 3A, in mice bearing bilateral MC38-derived tumors, CD8 T cells were an absolute requirement for the local tumor eradication and for the modest abscopal effects, while CD4 T cells were dispensable (figure 3B). Moreover, when similar experiments were performed in mice lacking cDC1 cells (BATF3$^{-/-}$ mice), the antitumor effects were completely abolished (figure 3C,D). Given the fact that BO-112 and RT both induce type I IFN, we also addressed if sensitivity to IFN α/ß by the tumor-bearing mouse was required. Indeed, the local and abscopal antitumor efficacy against MC38-derived tumors was lost in IFNAR$^{-/-}$ mice (figure 3E,F), as well as in the case of B16-OVA-derived bilateral tumors (online supplemental figure 3D,E).

Taking together, these results suggest that a prominent CD8-mediated antitumor immune response was exerting the antitumor therapeutic effects and more conspicuously so against the directly treated tumors.

RT changes the immune tissue microenvironment of irradiated tumor lesions and ipsilateral lymph nodes

Our observations of therapeutic effects on irradiated tumor lesions prompted us to carry out experiments to investigate changes in the immune context of the tumor microenvironment due both to irradiation and the intratumoral injection of BO-112. Accordingly, our 8 Gy fractionated doses on alternate days and repeated intratumoral BO-112 injections were applied to mice bearing bilateral B16-OVA-derived tumors. Tumors were surgically excised on day 19 when the effects on tumor size started to be macroscopically perceived (figure 4A,B) and cell suspensions from such tumors were analyzed by multicolor flow cytometry and multiplex immunofluorescence for the tumor tissue sections. The gating strategy to monitor live tumor cells is shown in online supplemental figure 6. Intratumoral BO-112 plus RT in such tumors showed evidence for synergistic effects since showing a statistically significant increase of CD8 T cells and cDC1 cells in irradiated tumor tissue compared with vehicle-treated control tumors (figure 4C,D). In contrast, the numbers of conventional CD4 T cells (CD4^{+}Foxp3^{-}) within the tumor microenvironment were not altered by the dual RT+BO-112 treatments (figure 4C,D).

Regarding the tumor-draining lymph nodes, absolute numbers of T lymphocyte subsets were also quantitated on day+19 in ipsilateral and contralateral tumor-draining lymph nodes. Flow cytometry analyses revealed that absolute numbers of CD8 T cells expressing granzyme B, Ki-67 and CD137 were statistically significant increase in the ipsilateral draining lymph nodes at those tumor sites receiving radiation and intratumoral BO-112 (figure 4E). Such changes were not observed in contralateral lymph nodes. However, MHC-tetramer staining to detect OVA-specific CD8+ T cells showed clear increases on combined therapy both in the treated and contralateral tumor draining limph nodes (TDLNs) (figure 4F). To assess if T cell recirculation was required for efficacy, experiments were performed on inhibition of the sphingosine 1-phosphate receptor with FTY720. As shown in online supplemental figure 5, FTY720 treatment abolished contralateral efficacy, while ipsilateral efficacy was preserved (online supplemental figure 7).

Moreover, analyses with an MHC multimer that detects specific CD8 T cells which recognize the OVA immunodominant antigen expressed by B16-OVA tumor cells showed a clear tendency for mice undergoing the combined treatment to host higher numbers of tumor-reactive CD8 T lymphocytes (figure 4F).

For functional evaluation of antigen-specific CD8 T cells (CTLs), in vivo killing experiments (figure 5A) were performed following the instigation of RT plus intratumoral injection of BO-112 into B16-OVA-derived tumors. Once treatment was completed, on day 19 mice were transferred with differentially CFSE-labeled splenocytes pulsed or not with the SIINFEKL peptide to test in vivo cytotoxicity on day 19. As shown in figure 5B, RT plus BO-112 resulted in more intense CTL activity directed to OVA as a subrogate tumor antigen in this experimental setting.

Irradiation and BO-112 treatment in one of the tumor lesions enhanced responses to RT in distant tumors not injected with BO-112

In the clinic, a frequent issue is in patients with multiple tumor lesions that can be irradiated, is that only one or a few are amenable to repeated intratumoral injections. In this context, we studied whether repeated injections of only one lesion would be conducive to responses to RT in non-injected lesions.

Experiments were carried out in mice bearing bilateral TS/A-derived tumors, as schematized in figure 6A. These experiments were performed in such a way that in some groups of mice the contralateral tumor also received the RT regimen. For comparison, control group mice received only vehicle treatment or combined RT plus BO-112 to both tumor lesions (figure 6B).

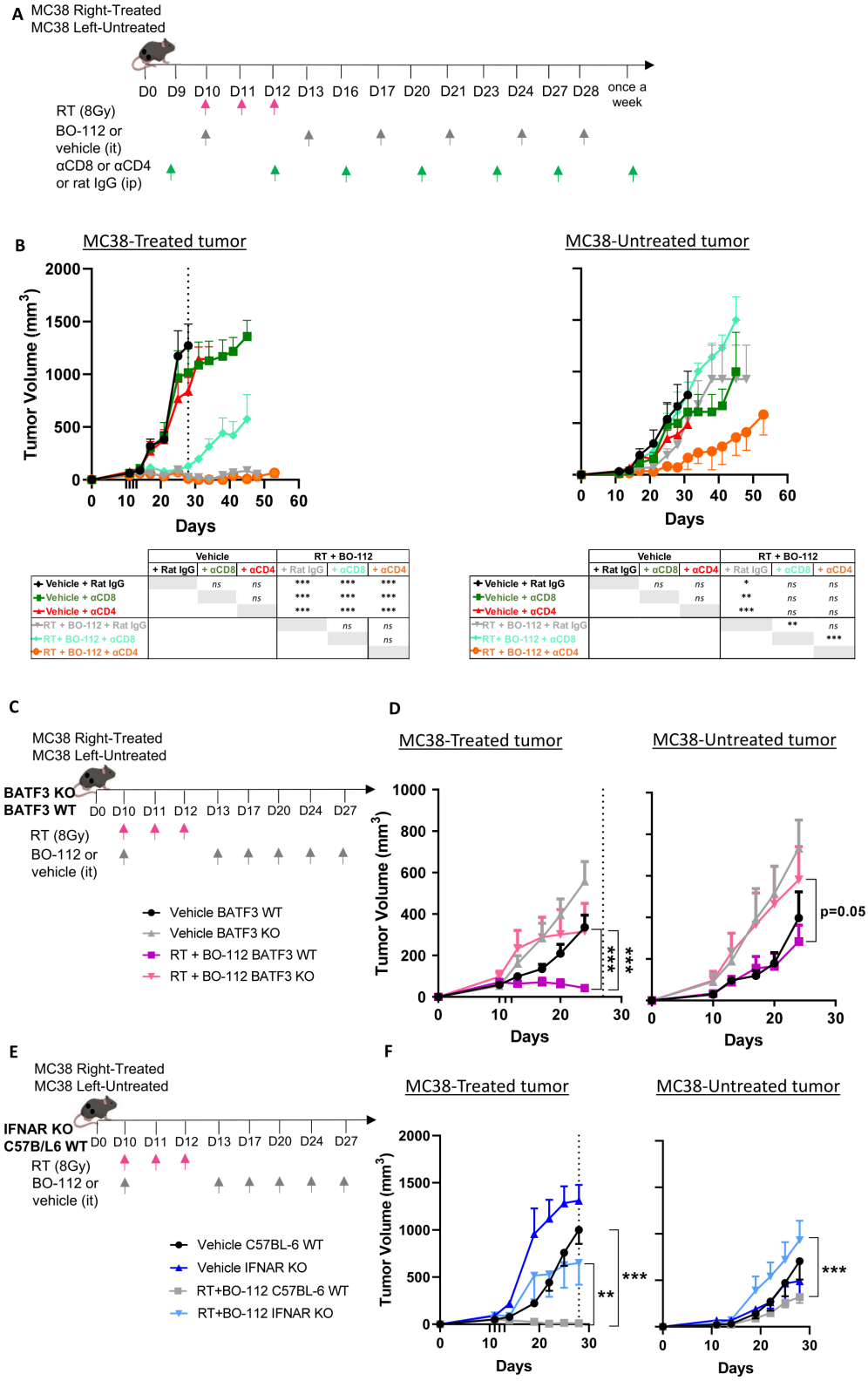

Figure 3 CD8 T cells, BATF-3–dependent dendritic cells and responsiveness to type I IFN were necessary for the local synergy of radiotherapy with BO-112. (A) Scheme of selective depletion of CD4 or CD8 T cells in mice bearing bilateral MC38-derived tumors in which one of the lesions was treated with radiotherapy and BO-112 as indicated. (B) Means±SEM of the size of tumors followed over time for the indicated color-coded groups. (C) Scheme of 10-day tumor engraftment and subsequent treatments with hypofractionated radiotherapy and intratumoral injections of BO-112 in bilateral subcutaneous MC38-derived tumors in BATF-3 KO mice whose size was monitored. BATF-3 WT mice were analyzed as control. Radiotherapy and BO-112 were given to the same tumor lesions. (D) Means±SEM and statistical comparisons among experimental groups ***p<0.001 (two-way ANOVA). Similar experiments in groups of BATF3 (C–D) and IFNAR KO (E–F) mice in comparison to co-housed WT C57BL/6 control mice. IFNAR, interferon-α/β receptor; KO, knockout; WT, wild type.

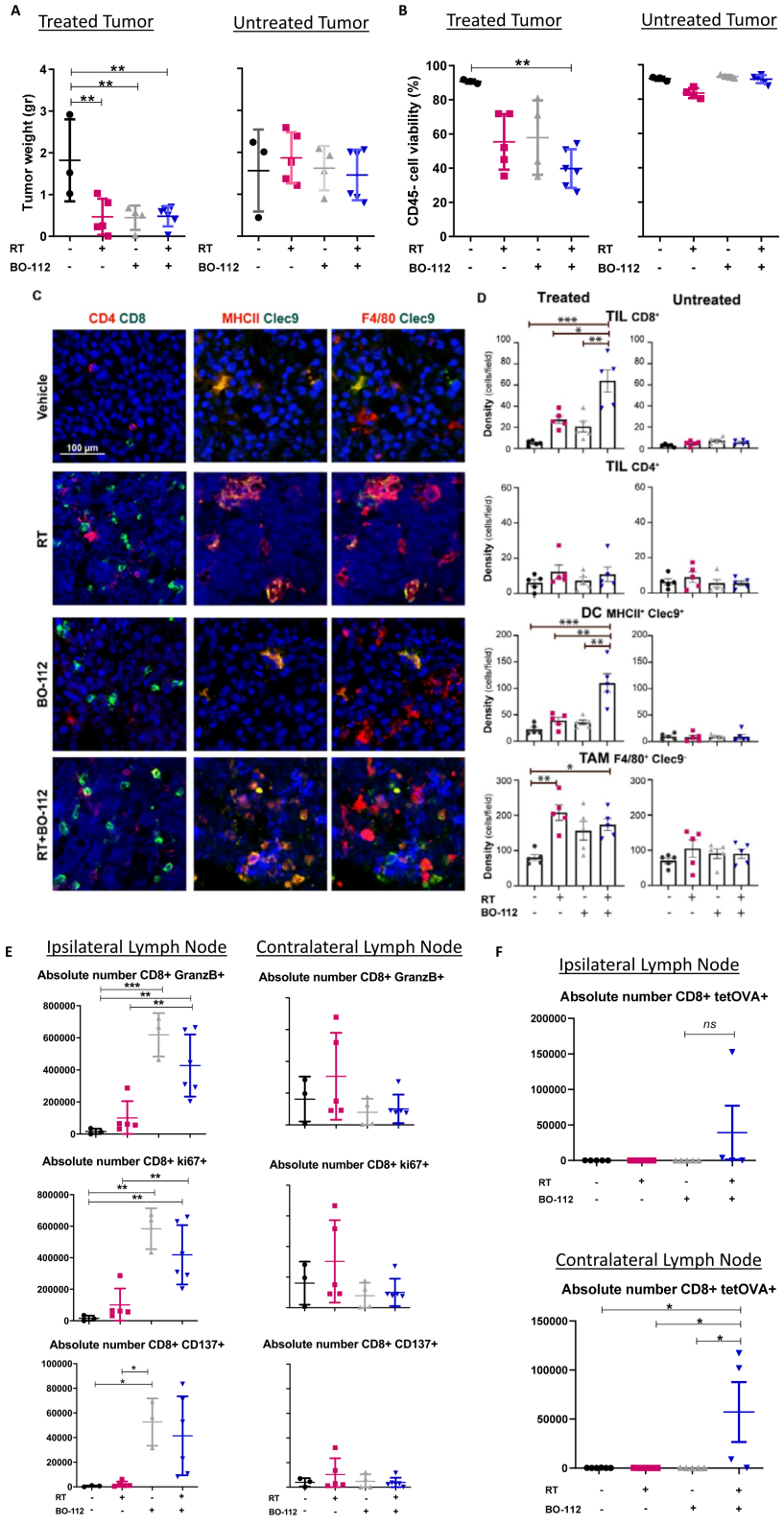

Figure 4 Radiotherapy in combination with intratumoral BO-112 enhances CD8 T-cell content in treated tumors and tumor draining lymph nodes. (A) Tumor weight of treated and untreated tumors 5 days after RT treatment. (B) Cell viability of treated and untreated malignant cells in the tumors 5 days after RT treatment. (C) Representative confocal images of B16-OVA-treated tumors as indicated. Bar, 100 µm. 20× fields. (D) Plots showing the respective densities of CD8+ and CD4+ lymphocytes, type-1 DCs (MHCII+CLEC9+) and TAM (F4/80+CLEC9–) in treated and untreated tumors, as indicated. Statistical comparisons were performed using one-way ANOVA test with Tukey post-test analysis (*p<0.05). Mean±SEM. (E) Plots representing the absolute numbers of the indicated T-cell subsets in the treated tumor-draining lymph nodes or the contralateral lymph nodes. (F) Results as in D representing OVA-specific CD8 T cells by H-2K^{b} tetramer staining. Statistical comparisons between different groups were performed using one-way ANOVA. Mean±SEM; *p<0.05, **p<0.01, ***p<0.001. n=4–6 mice/group. RT, radiotherapy.

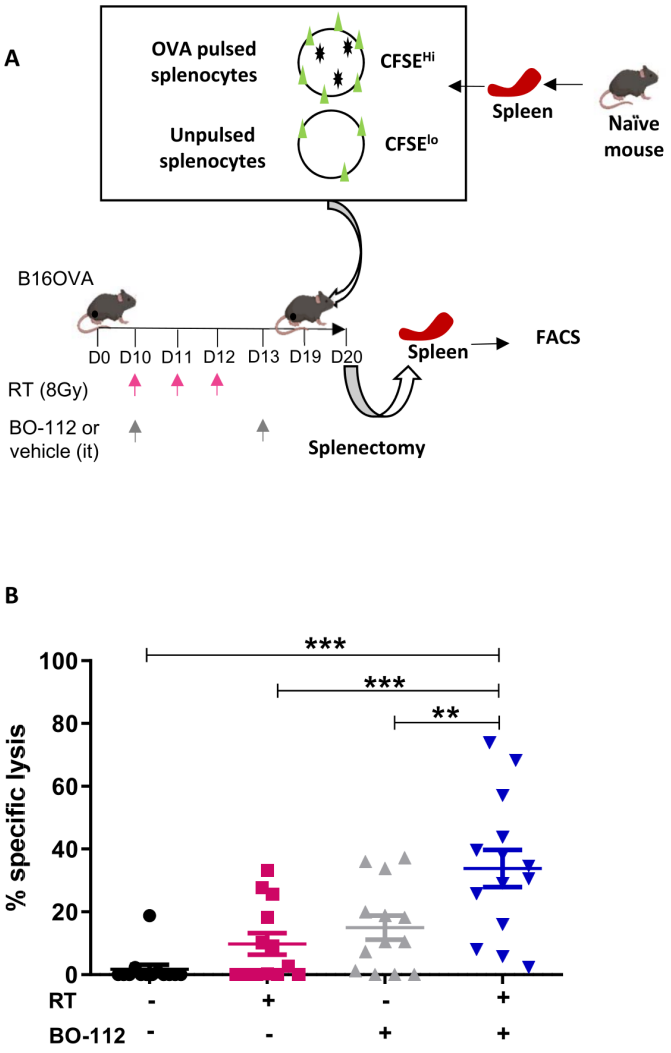

Figure 5 Combined radiotherapy and BO-112 local treatment induces systemic antitumor antigen-specific cytotoxicity. (A) Schematic representation of in vivo killing assays in mice bearing bilateral B16-OVA tumors treated as indicated and subjected on day 19 to classic in vivo cytotoxicity assays to SINFEKL peptide-pulsed target splenocytes at day 19. (B) Percentage of in vivo specific anti-ova cytotoxicity in the indicated treatment groups of mice is shown. Statistical comparisons between groups were performed using two-way ANOVA. Mean±SEM; **p<0.01, ***p<0.001

Interestingly, the efficacy of RT on the contralateral non-injected tumor lesions was increased leading to complete rejections in 10 out of 10 treated mice. This level of bilateral efficacy was comparable to the efficacy attained when both lesions received the combined treatment (figure 6C,D). These results are compatible with the feasible clinical management of oligometastatic disease.

Reportedly, low-dose RT may result in immune-mediated antitumor effects in radioimmunotherapy combinations.[41] However, in our experimental system such low-dose irradiation regimens (1 Gy/3 fractions) failed to synergize with intratumoral BO-112 even when given to both coexisting transplanted tumors (online supplemental figure 8).

DISCUSSION

Radioimmunotherapy is considered a promising research field to increase treatment efficacy in patients with cancer.[42 43] In this study, we investigated the feasibility and efficacy of a local immunotherapy treatment given in combination with external beam irradiation. Stereotactic ablative RT was chosen as a clinically feasible RT approach given at 3 fractions of 8 Gy doses. Such non-ablative suboptimal doses were chosen based on evidence for the greater proimmunogenic effects in mouse models when using such an RT regimen.[44] Other investigators have reported effects of low-dose RT doses,[41] but in our combined regimens we do not observe synergy at such dose levels.

Conceivably, the immunogenicity of tumor cell death elicited by ionizing radiation[45] can be enhanced by pathogen-associated molecular patterns[46] that mimic viral infection. This was the rationale for combining radiation with a nanoplexed form of poly I:C that mimics a tumor tissue infection by a double-stranded RNA virus. In such an experimental setting, cell death will cause the release of tumor-associated antigens to be uptaken by dendritic cells and cross-presented to T cells. Importantly, both elements in the combination (tumor cell death from RT and BO-112) would lead to dendritic cell activation/maturation. In these combined schemes, we intend to set in motion innate and adaptive immunity mechanisms that would result in meaningful antitumor efficacy.

Ex vivo experiments with tumor cell lines indicated that the combination of irradiation and BO-112 indeed produced more pronounced hallmarks of immunogenic cell death.[23] In vivo, very clear signs of synergistic efficacy were observed against the treated tumor but not so clearly, and much more modestly, against concomitant untreated lesions. It is becoming clear that abscopal effects against macroscopic disease are difficult to attain in the clinic. However, our quadruple combination regimen consisting of RT+BO-112 intratumoral+anti-PD-1+anti-CTLA-4 consistently delayed contralateral tumor progression.

The mechanism behind the excellent local tumor control was clearly immune-mediated and contingent on CD8-mediated adaptive immune responses. In keeping with this notion, the function of type I IFN and cDC1 cells was absolutely needed and consistent with more prominent CD8 T-cell infiltrates in the tumors.[47] The reason for weak control of distant lesions in the presence of CD8 T-cell responses remains to be clarified. Our in vivo cytotoxicity results suggest problems in T-cell trafficking to non-irradiated sites and these mechanisms are currently under investigation. It is clear that the role of tumor antigen cross-presentation deserves more attention to understand how RT shapes antitumor T-cell immunity. The role of the type-1 interferon system in the process seems to be crucial.

Modest abscopal effects could be considered a disadvantage for a local immunotherapy plus an RT approach, in that it would perhaps only be applicable in the clinic to irresectable locally advanced tumors. However, we

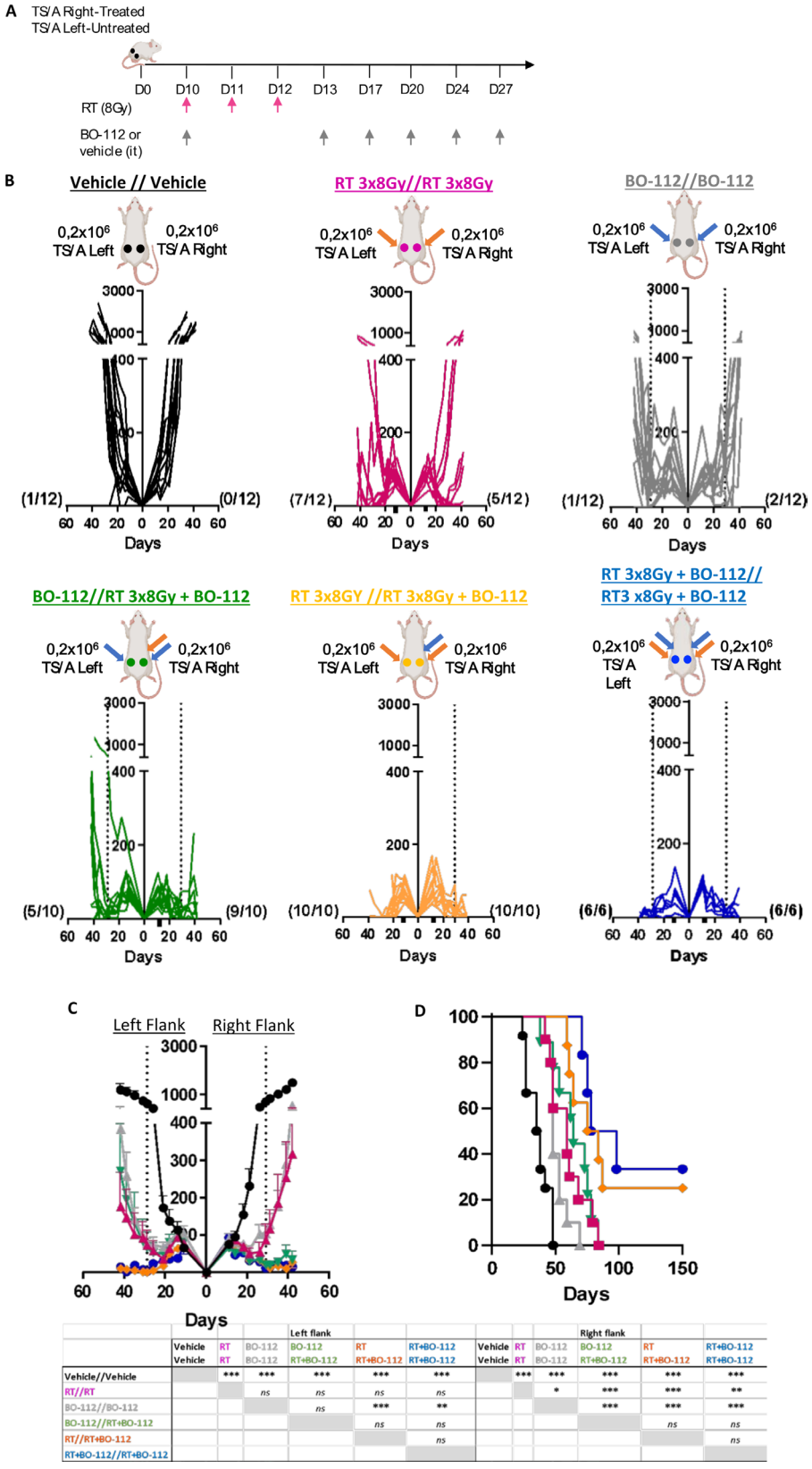

	Left flank						Right flank					
	Vehicle Vehicle	RT RT	BO-112 BO-112	BO-112 RT+BO-112	RT RT+BO-112	RT+BO-112 RT+BO-112	Vehicle Vehicle	RT RT	BO-112 BO-112	BO-112 RT+BO-112	RT RT+BO-112	RT+BO-112 RT+BO-112
Vehicle//Vehicle		***	***	***	***	***		***	***	***	***	***
RT//RT			ns	ns	ns	ns			*	***	***	**
BO-112//BO-112				ns	***	**				***	***	***
BO-112//RT+BO-112					ns	ns					ns	ns
RT//RT+BO-112						ns						ns
RT+BO-112//RT+BO-112												

Figure 6 Irradiation and BO-112 treatment of one tumor lesion sensitize distant lesions to radiotherapy. (A) Schematic representation of treatment in groups of mice bearing bilateral TS/A-derived tumors in which one of the tumor lesions received radiotherapy and/or intratumoral BO-112, while the contralateral tumors remained untreated or received only radiotherapy. (B) Individual follow-up of bilateral tumor sizes in mice receiving the indicated treatments in their right or left tumors. The dotted line indicates the last intratumoral injection of BO-112. (C) Mean±SEM of tumor sides in the groups of mice in B with statistical comparisons and (D) the Kaplan-Meier graph observed survival over time. A two-way ANOVA test was used to assess significance. Significant differences are displayed for comparisons with different groups *p<0.05, **p<0.01, ***p<0.001.

also tested and modeled a frequent clinical condition in which patients present with multiple oligometastatic macroscopic lesions that are amenable to RT but in which only one or two of those metastases are suitable for intratumoral injections. In these settings, irradiation of all tumors is usually feasible and our experiments suggest that BO-112 administered to only one of the lesions was capable of inducing a rescuing response in the non-injected tumor sites. However, these oligometastatic patients still represent a minority of the cases and preclinical research should address this point to bring benefit to patients with more spread disease. In our opinion, multiple agent combinations will be required to reach meaningful efficacy in such cases.[48]

RT is a formidable tool for the management of patients with oligometastatic cancer prolonging overall survival.[49] Our data suggest that such strategies can benefit from safe image-guided local interventions to deliver immunotherapy agents. Schemes of treatment can be devised by irradiating as many metastases as possible, while injecting only some of them with intratumoral doses of BO-112, perhaps combined with PD(L)1 blockade and/or anti-CTLA-4 mAbs.

A clinical trial with such a design for patients with oligometastatic NSCLC is ongoing at our institution (Eudract 2021-006410-36). Intratumoral BO-112 has shown efficacy in a single-arm phase II trial in patients with melanoma refractory to PD-1 agents, reaching an ORR (overall rate response) of 30% when used in combination with pembrolizumab.[9] This profile suggests that intratumoral BO-112 is among the best intratumoral immunotherapy agents as had also been previously documented in mouse models.[13] In this regard, co-injection of BO-112 with other pathogen-associated molecular patterns might be advisable as already shown by coinjection with STING agonists.[14]

Our preclinical data provide compelling evidence for synergy against solid malignancies that are directly treated by irradiation and BO-112. In some cases, those local effects of RT might be critical for therapeutic and palliative care. Therefore, the combination of RT with local immunotherapy agents such as BO-112 holds much promise for clinical translation.

Author affiliations
[1]Program of Immunology and Immunotherapy, Center for Applied Medical Research (CIMA), Pamplona, Spain
[2]Navarra Institute for Health Research (IDISNA), Pamplona, Spain
[3]Departments of Immunology-Immunotherapy and Oncology, Clínica Universidad de Navarra, Pamplona, Spain
[4]Centro de Investigación Biomédica en Red de Cáncer (CIBERONC), Madrid, Spain
[5]Departments of immunology and pathology, Hospital Gregorio Marañon, Madrid, Spain
[6]Departments of medical physic, Clínica Universidad de Navarra, Pamplona, Spain
[7]Highlight Therapeutics, Valencia, Spain

Twitter Eneko Garate-Soraluze @garateeneko and Celia Barrio-Alonso @isgonnabethecel

Acknowledgements We are grateful to D Alignani from the flow cytometry facility and to Eneko Elizalde and Elena Ciordia from the animal facility for their excellent work. Drs Martinez-Monge, Aranda and Berraondo are acknowledged for helpful discussions. Excellent dosimetry by Haizea Etxeberria is also acknowledged. English editing by Paul Miller and project management by E Guirado and B Palencia are much appreciated.

Contributors MER-R performed experiments, analyzed results, designed research, wrote the manuscript, provided funding and is guarantor. IS-M, PS-M, IRL, MA performed experiments and analyzed results. EG-S performed experiments. CB-A, VDP, LAM, MFS, JLP-G, HE-O and MQ analyzed results. IM designed research, analyzed results, wrote the manuscript and provided funding.

Funding This work has been supported by the Cancer Research UK (C18915/A29362), FCAECC and AIRC under the Accelerator Award Programme, Proyecto RTC2019- 006860-1 financiado por MCIN/AEI /10.13039/501100011033, the Instituto de Salud Carlos III (ISCIII) through the project PI20/00434 and co-funded by the European Union. MER-R is supported by the Fundación CRIS, Programa Talento Clínico 2020 (PR_TCL_2020-03). MFS is supported by a Miguel Servet contract MS17/00196 and a grant project PI19/00668 from Instituto de Salud Carlos III, Fondo de Investigacion Sanitaria (Spain).

Competing interests IS-M, EG-S, VDP, LAM, JLP-G, MA, CB-A and PS-M declare no competing interests. MER-R reports receiving research funding from Roche and Highlight Therapeutics. She also has received speaker's bureau honoraria from BMS and ROCHE. MFS reports receiving research funding from Roche. MQ and HE-O, CEO and full-time employee of Highlight Therapeutics, respectively. IM reports receiving commercial research grants from BMS, Highlight Therapeutics, Alligator, Pfizer Genmab and Roche; has received speaker's bureau honoraria from MSD; and is a consultant or advisory board member for BMS, Roche, AstraZeneca, Genmab, Pharmamar, F-Star, Bioncotech, Bayer, Numab, Pieris, Gossamer, Alligator and Merck Serono.

Patient consent for publication Not applicable.

Ethics approval Not applicable.

Provenance and peer review Not commissioned; externally peer reviewed.

Data availability statement All data relevant to the study are included in the article or uploaded as supplementary information. Data will be shared upon reasonable request to authors.

ORCID iDs
Maria E Rodriguez-Ruiz http://orcid.org/0000-0002-9765-2499
Celia Barrio-Alonso http://orcid.org/0000-0002-2789-1363
Maite Alvarez http://orcid.org/0000-0002-5969-9181
Ignacio Melero http://orcid.org/0000-0002-1360-348X

REFERENCES

1 Marabelle A, Tselikas L, de Baere T, *et al*. Intratumoral immunotherapy: using the tumor as the remedy. *Ann Oncol* 2017;28:xii33–43.
2 Melero I, Castanon E, Alvarez M, *et al*. Intratumoural administration and tumour tissue targeting of cancer immunotherapies. *Nat Rev Clin Oncol* 2021;18:558–76.
3 Ressler JM, Karasek M, Koch L, *et al*. Real-life use of talimogene laherparepvec (T-VEC) in melanoma patients in centers in Austria, Switzerland and Germany. *J Immunother Cancer* 2021;9.
4 Henderson GB, Ulrich P, Fairlamb AH, *et al*. "Subversive" substrates for the enzyme trypanothione disulfide reductase: alternative

approach to chemotherapy of Chagas disease. *Proc Natl Acad Sci U S A* 1988;85:5374–8.
5 Frank MJ, Reagan PM, Bartlett NL, *et al*. In Situ Vaccination with a TLR9 Agonist and Local Low-Dose Radiation Induces Systemic Responses in Untreated Indolent Lymphoma. *Cancer Discov* 2018;8:1258–69.
6 Bauer S, Wagner H. Bacterial CpG-DNA licenses TLR9. *Curr Top Microbiol Immunol* 2002;270:145–54.
7 Kyi C, Roudko V, Sabado R, *et al*. Therapeutic immune modulation against solid cancers with intratumoral Poly-ICLC: a pilot trial. *Clin Cancer Res* 2018;24:4937–48.
8 Márquez-Rodas I, Longo F, Rodriguez-Ruiz ME, *et al*. Intratumoral nanoplexed poly I:C BO-112 in combination with systemic anti-PD-1 for patients with anti-PD-1-refractory tumors. *Sci Transl Med* 2020;12. doi:10.1126/scitranslmed.abb0391. [Epub ahead of print: 14 Oct 2020].
9 Rodríguez-Moreno J, Dutriaux C, Merino LdelaC, *et al*. Preliminary results of a phase 2 study of intratumoral administration of bo-112 with pembrolizumab in patients with advanced melanoma that have progressive disease on anti-pd-1-based therapy. *Journal for ImmunoTherapy of Cancer* 2021;9:A1011–2.
10 1057P - ROS1 mutation can serve- as a potential efficacious predictor of immunotherapy in melanoma patients. *Annals of Oncology* 2021;32:S867–905.
11 Tormo D, Checińska A, Alonso-Curbelo D, *et al*. Targeted activation of innate immunity for therapeutic induction of autophagy and apoptosis in melanoma cells. *Cancer Cell* 2009;16:103–14.
12 Kalbasi A, Tariveranmoshabad M, Hakimi K, *et al*. Uncoupling interferon signaling and antigen presentation to overcome immunotherapy resistance due to JAK1 loss in melanoma. *Sci Transl Med* 2020;12. doi:10.1126/scitranslmed.abb0152. [Epub ahead of print: 14 Oct 2020].
13 Aznar MA, Planelles L, Perez-Olivares M, *et al*. Immunotherapeutic effects of intratumoral nanoplexed poly I:C. *J Immunother Cancer* 2019;7:116.
14 Alvarez M, Molina C, De Andrea CE, *et al*. Intratumoral co-injection of the poly I:C-derivative BO-112 and a STING agonist synergize to achieve local and distant anti-tumor efficacy. *J Immunother Cancer* 2021;9:e002953.
15 Demaria S, Golden EB, Formenti SC. Role of local radiation therapy in cancer immunotherapy. *JAMA Oncol* 2015;1:1325–32.
16 Stone HB, Peters LJ, Milas L. Effect of host immune capability on radiocurability and subsequent transplantability of a murine fibrosarcoma. *J Natl Cancer Inst* 1979;63:1229–35.
17 Bloy N, Pol J, Manic G, *et al*. Trial watch: radioimmunotherapy for oncological indications. *Oncoimmunology* 2014;3:e954929.
18 Golden EB, Apetoh L. Radiotherapy and immunogenic cell death. *Semin Radiat Oncol* 2015;25:11–17.
19 Castedo M, Coquelle A, Vivet S, *et al*. Apoptosis regulation in tetraploid cancer cells. *Embo J* 2006;25:2584–95.
20 Deng L, Liang H, Burnette B, *et al*. Irradiation and anti-PD-L1 treatment synergistically promote antitumor immunity in mice. *J Clin Invest* 2014;124:687–95.
21 Segura E, Amigorena S. Cross-Presentation in mouse and human dendritic cells. *Adv Immunol* 2015;127:1–31.
22 Rodriguez-Ruiz ME, Rodriguez I, Garasa S, *et al*. Abscopal effects of radiotherapy are enhanced by combined immunostimulatory mAbs and are dependent on CD8 T cells and Crosspriming. *Cancer Res* 2016;76:5994–6005.
23 Galluzzi L, Buqué A, Kepp O, *et al*. Immunogenic cell death in cancer and infectious disease. *Nat Rev Immunol* 2017;17:97–111.
24 Mondini M, Levy A, Meziani L, *et al*. Radiotherapy-immunotherapy combinations - perspectives and challenges. *Mol Oncol* 2020;14:1529–37.
25 Luke JJ, Lemons JM, Karrison TG, *et al*. Safety and clinical activity of pembrolizumab and multisite stereotactic body radiotherapy in patients with advanced solid tumors. *J Clin Oncol* 2018;36:1611–8.
26 Formenti SC, Rudqvist N-P, Golden E, *et al*. Radiotherapy induces responses of lung cancer to CTLA-4 blockade. *Nat Med* 2018;24:1845–51.
27 Demaria S, Kawashima N, Yang AM, *et al*. Immune-mediated inhibition of metastases after treatment with local radiation and CTLA-4 blockade in a mouse model of breast cancer. *Clin Cancer Res* 2005;11:728–34.
28 Twyman-Saint Victor C, Rech AJ, Maity A, *et al*. Radiation and dual checkpoint blockade activate non-redundant immune mechanisms in cancer. *Nature* 2015;520:373–7.
29 Sato H, Demaria S, Ohno T. The role of radiotherapy in the age of immunotherapy. *Jpn J Clin Oncol* 2021;51:513–22.
30 Brody JD, Goldstein MJ, Czerwinski DK, *et al*. Immunotransplantation preferentially expands T-effector cells over T-regulatory cells and cures large lymphoma tumors. *Blood* 2009;113:85–94.
31 Kim YH, Gratzinger D, Harrison C, *et al*. In situ vaccination against mycosis fungoides by intratumoral injection of a TLR9 agonist combined with radiation: a phase 1/2 study. *Blood* 2012;119:355–63.
32 Brody JD, Ai WZ, Czerwinski DK, *et al*. In situ vaccination with a TLR9 agonist induces systemic lymphoma regression: a phase I/II study. *J Clin Oncol* 2010;28:4324–32.
33 Demaria S, Vanpouille-Box C, Formenti SC, *et al*. The TLR7 agonist imiquimod as an adjuvant for radiotherapy-elicited in situ vaccination against breast cancer. *Oncoimmunology* 2013;2:e25997.
34 Dewan MZ, Vanpouille-Box C, Kawashima N, *et al*. Synergy of topical toll-like receptor 7 agonist with radiation and low-dose cyclophosphamide in a mouse model of cutaneous breast cancer. *Clin Cancer Res* 2012;18:6668–78.
35 Hammerich L, Marron TU, Upadhyay R, *et al*. Systemic clinical tumor regressions and potentiation of PD1 blockade with in situ vaccination. *Nat Med* 2019;25:814–24.
36 Rodríguez-Ruiz ME, Perez-Gracia JL, Rodríguez I, *et al*. Combined immunotherapy encompassing intratumoral poly-ICLC, dendritic-cell vaccination and radiotherapy in advanced cancer patients. *Ann Oncol* 2018;29:1312–9.
37 Franken NAP, Rodermond HM, Stap J, *et al*. Clonogenic assay of cells in vitro. *Nat Protoc* 2006;1:2315–9.
38 Rodriguez-Ruiz ME, Buqué A, Hensler M, *et al*. Apoptotic caspases inhibit abscopal responses to radiation and identify a new prognostic biomarker for breast cancer patients. *Oncoimmunology* 2019;8:e1655964.
39 Panaretakis T, Kepp O, Brockmeier U, *et al*. Mechanisms of pre-apoptotic calreticulin exposure in immunogenic cell death. *Embo J* 2009;28:578–90.
40 Kubli SP, Berger T, Araujo DV, *et al*. Beyond immune checkpoint blockade: emerging immunological strategies. *Nat Rev Drug Discov* 2021;20:899–919.
41 Herrera FG, Ronet C, Ochoa de Olza M, *et al*. Low-Dose radiotherapy reverses tumor immune desertification and resistance to immunotherapy. *Cancer Discov* 2022;12:108–33.
42 Marciscano AE, Walker JM, McGee HM, *et al*. Incorporating radiation oncology into immunotherapy: proceedings from the ASTRO-SITC-NCI immunotherapy workshop. *J Immunother Cancer* 2018;6:6.
43 Formenti SC, Demaria S. Future of radiation and immunotherapy. *Int J Radiat Oncol Biol Phys* 2020;108:3–5.
44 Dewan MZ, Galloway AE, Kawashima N, *et al*. Fractionated but not single-dose radiotherapy induces an immune-mediated abscopal effect when combined with anti-CTLA-4 antibody. *Clin Cancer Res* 2009;15:5379–88.
45 Rodriguez-Ruiz ME, Vitale I, Harrington KJ, *et al*. Immunological impact of cell death signaling driven by radiation on the tumor microenvironment. *Nat Immunol* 2020;21:120–34.
46 Garg AD, Galluzzi L, Apetoh L, *et al*. Molecular and translational classifications of DAMPs in immunogenic cell death. *Front Immunol* 2015;6:588.
47 Sánchez-Paulete AR, Cueto FJ, Martínez-López M, *et al*. Cancer immunotherapy with immunomodulatory Anti-CD137 and anti-PD-1 monoclonal antibodies requires BATF3-Dependent dendritic cells. *Cancer Discov* 2016;6:71–9.
48 Sanmamed MF, Berraondo P, Rodriguez-Ruiz ME, *et al*. Charting roadmaps towards novel and safe synergistic immunotherapy combinations. *Nat Cancer* 2022;3:665–80.
49 Gutiontov SI, Pitroda SP, Tran PT, *et al*. (Oligo)metastasis as a Spectrum of Disease. *Cancer Res* 2021;81:2577–83.

Supplemental Figure 1

A

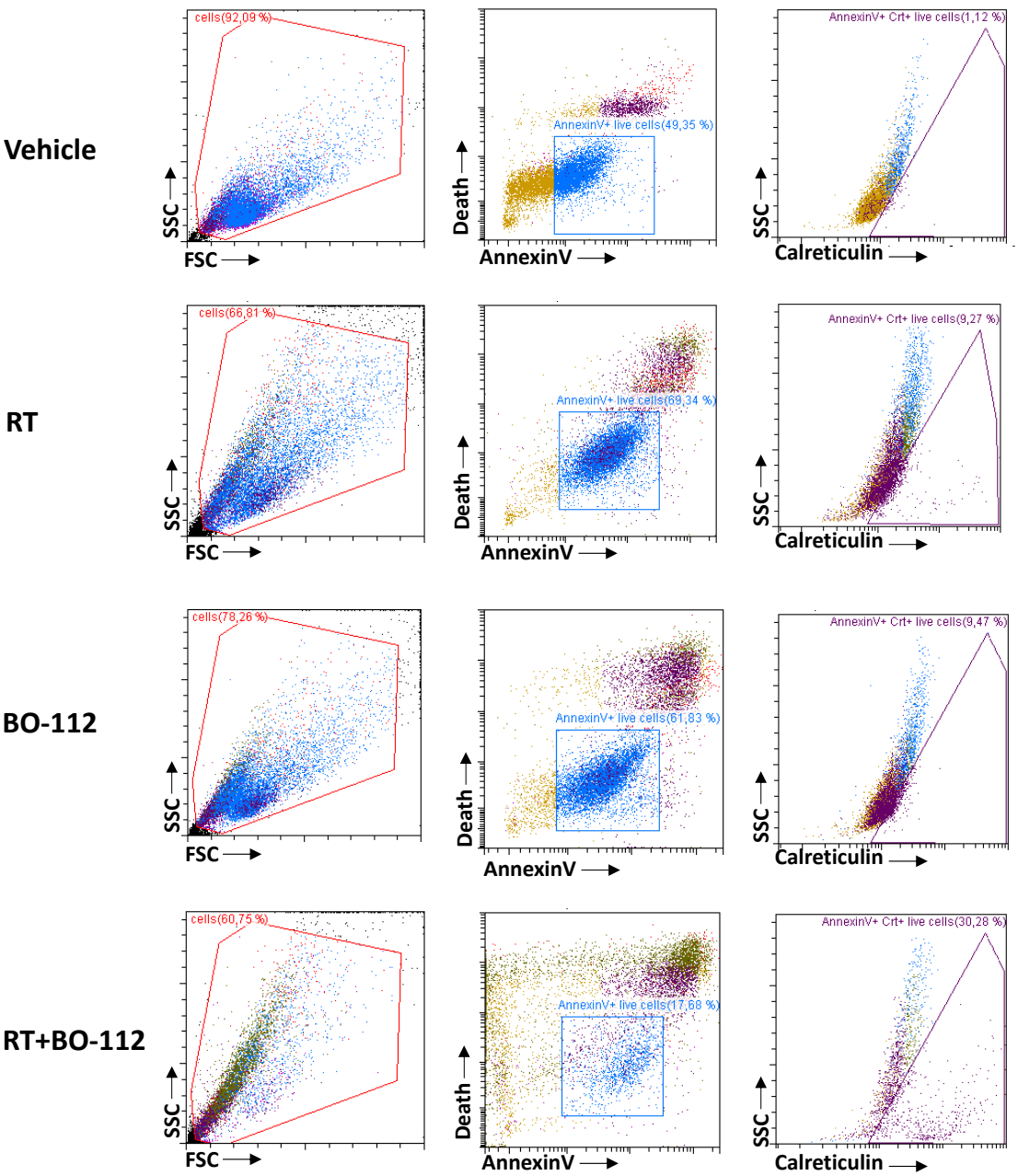

Supplemental Figure 2

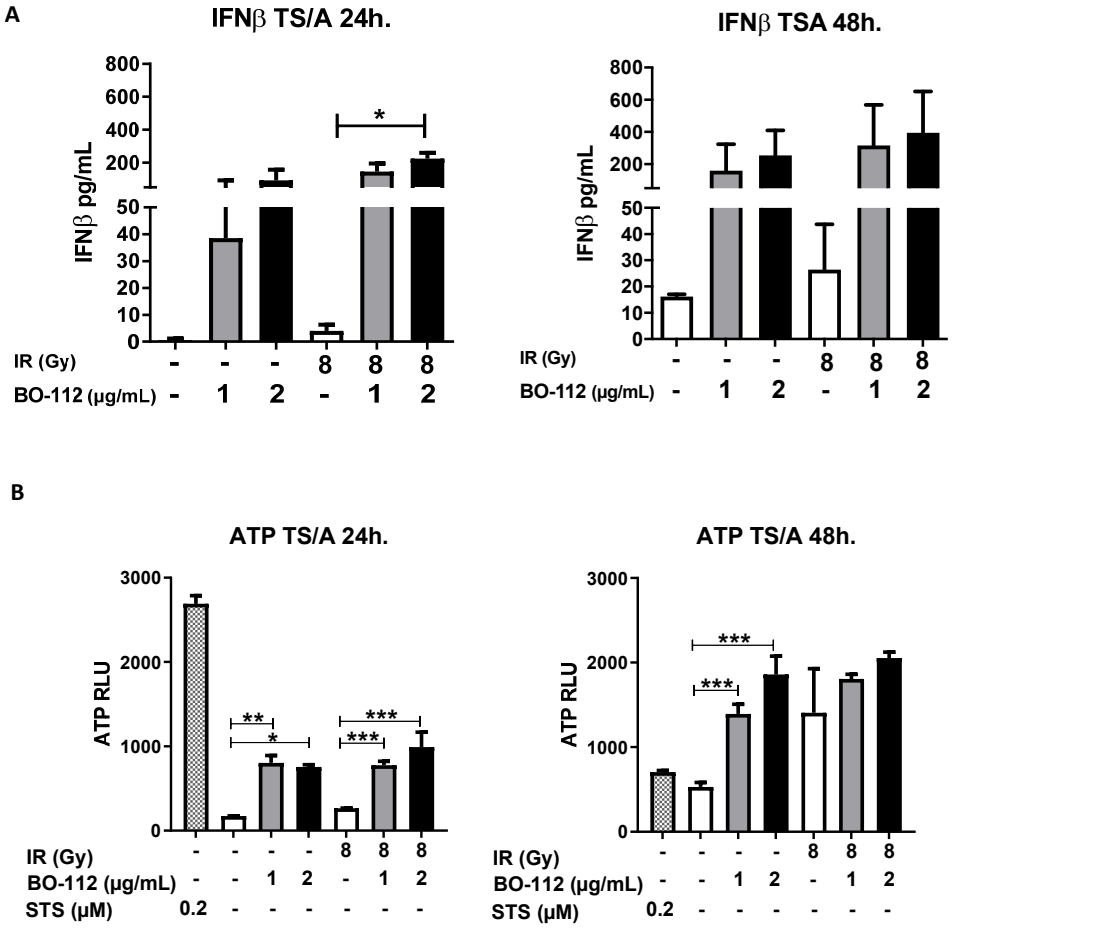

Supplemental Figure 3

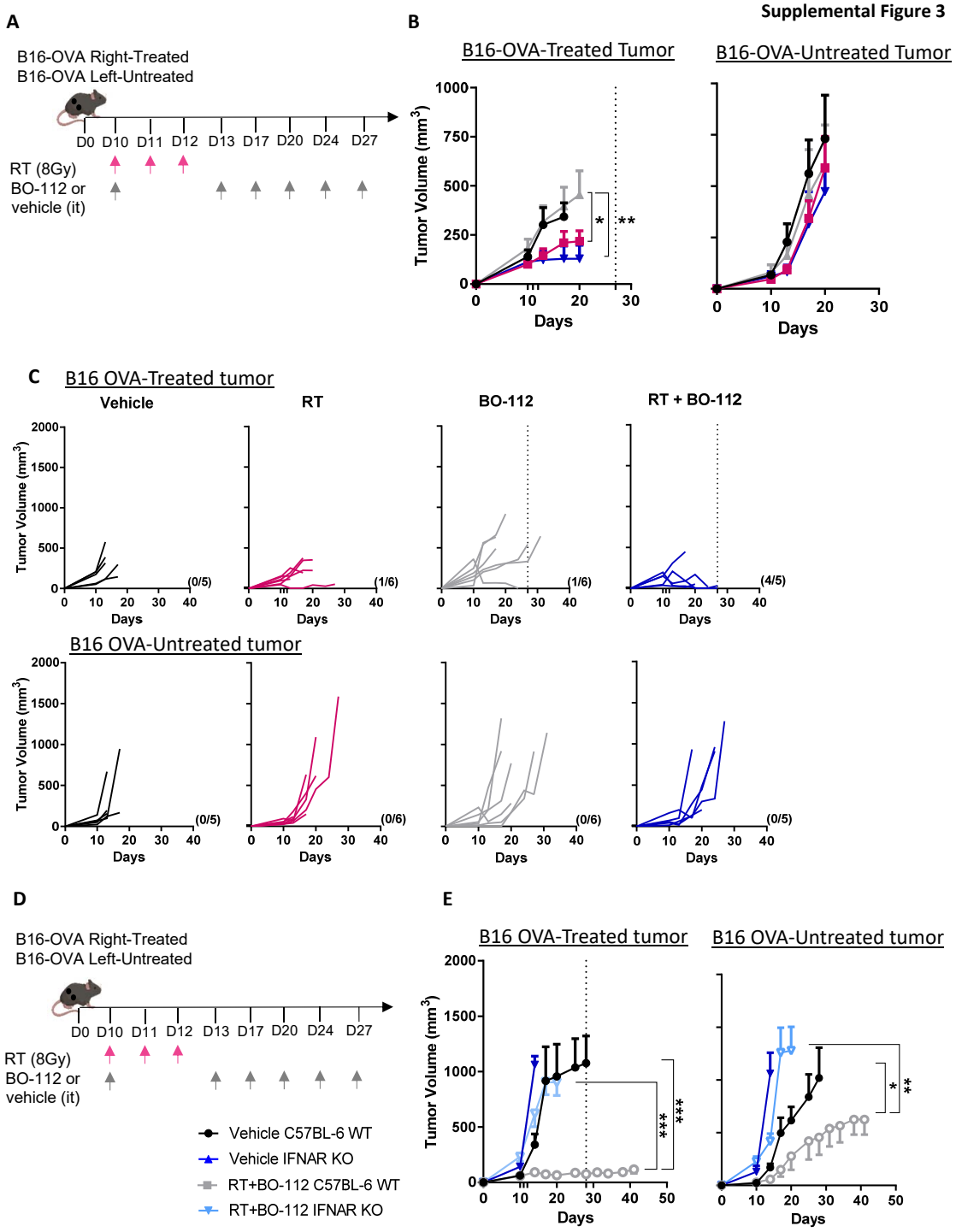

Supplemental Figure 4

A

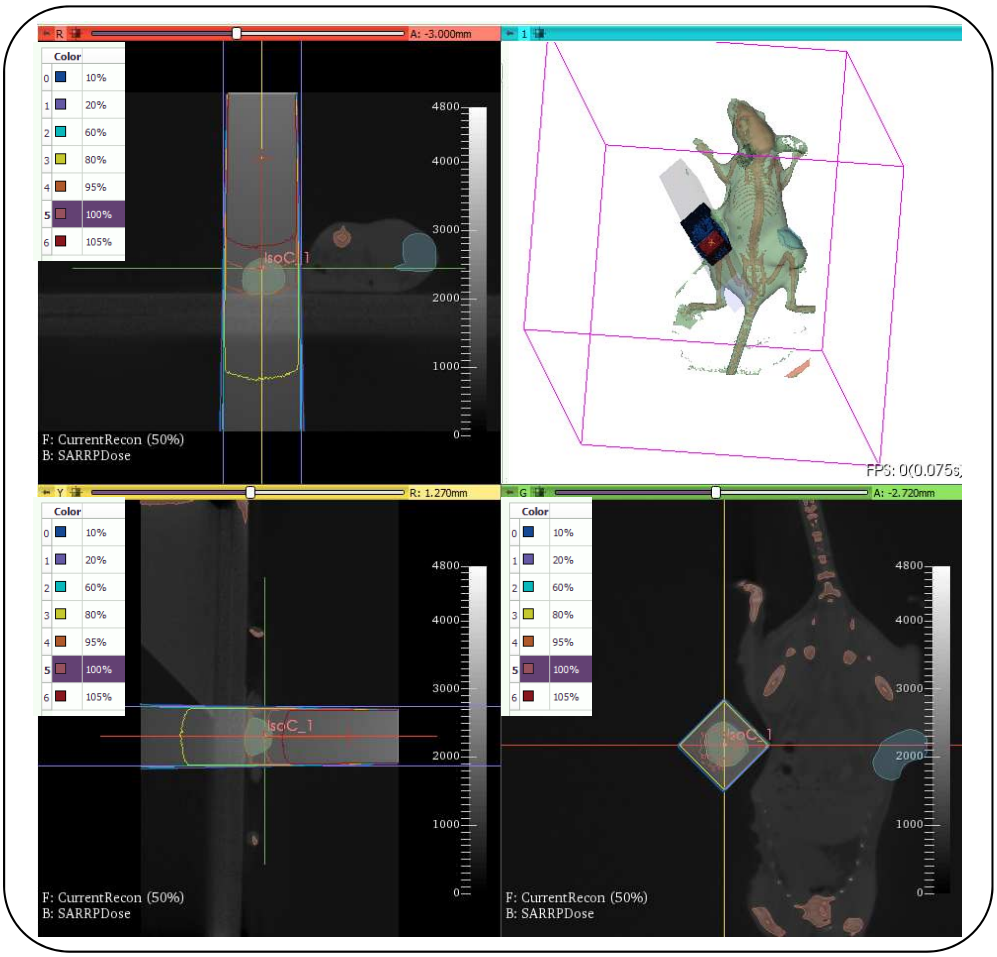

B

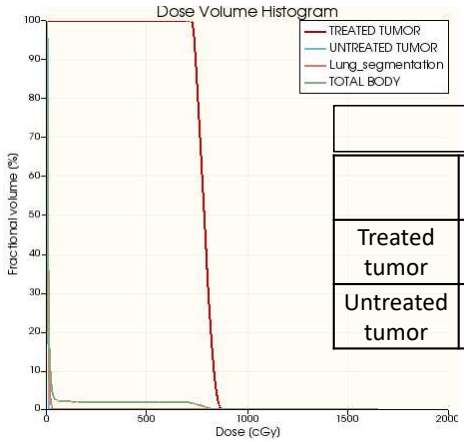

Relative dose				
	Volume(cc)	Mean(cGy)	Min(cGy)	Max(cGy)
Treated tumor	0.22	2354.05	1444.1	2466.35
Untreated tumor	0.19	5.61	1.70	12.79

Supplemental Figure 5

A

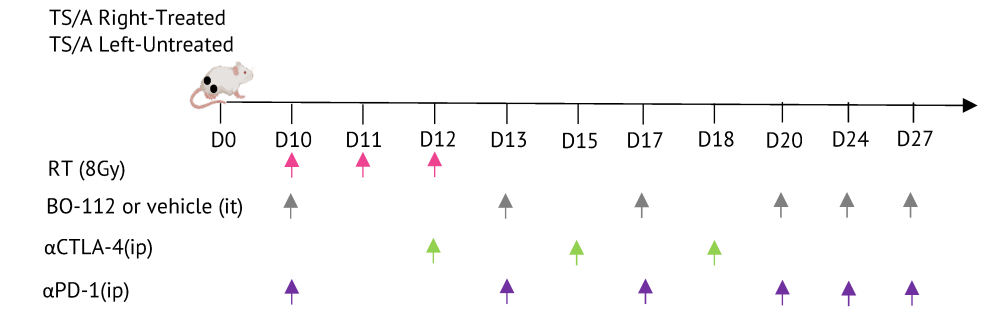

B

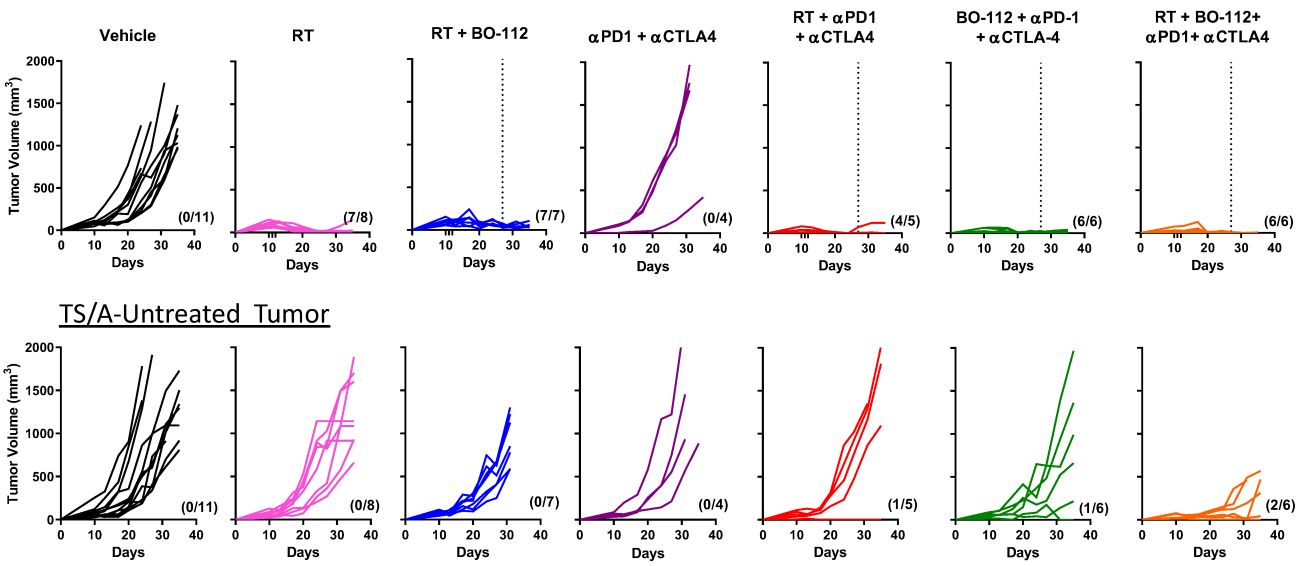

C

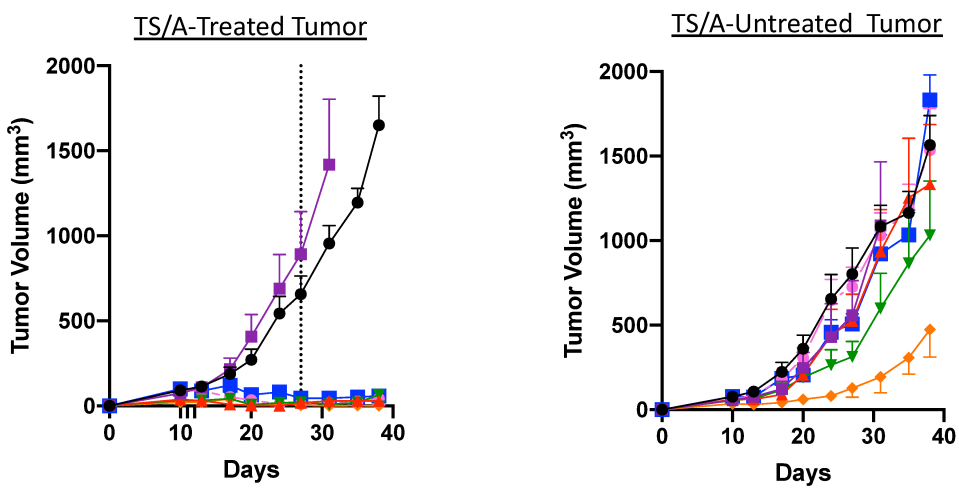

	Treated tumor							Untreated tumor						
	Vehicle	RT	RT+BO-112	PD1+CTLA4	RT+PD1 +CTLA4	BO-112 +PD1+CTLA4	RT+BO-112 +PD1+CTLA4	Vehicle	RT	RT+BO-112	PD1+CTLA4	RT+PD1 +CTLA4	112+PD1+ CTLA4	RT+BO-112 +PD1+CTLA4
Vehicle		***	***	*ns*	***	***	***		*ns*	*ns*	*ns*	*ns*	*ns*	***
RT			*ns*	***	*ns*	*ns*	*ns*			*ns*	*ns*	*ns*	*ns*	***
RT+BO-112				***	*ns*	*ns*	*ns*				*ns*	*ns*	*ns*	***
PD1+CTLA4					***	***	***					*ns*	*ns*	***
RT+PD1+CTLA4						*ns*	*ns*						**	***
BO-112+PD1+CTLA4							*ns*							*
RT+BO-112+PD1+CTLA4														

Supplemental Figure 6

A

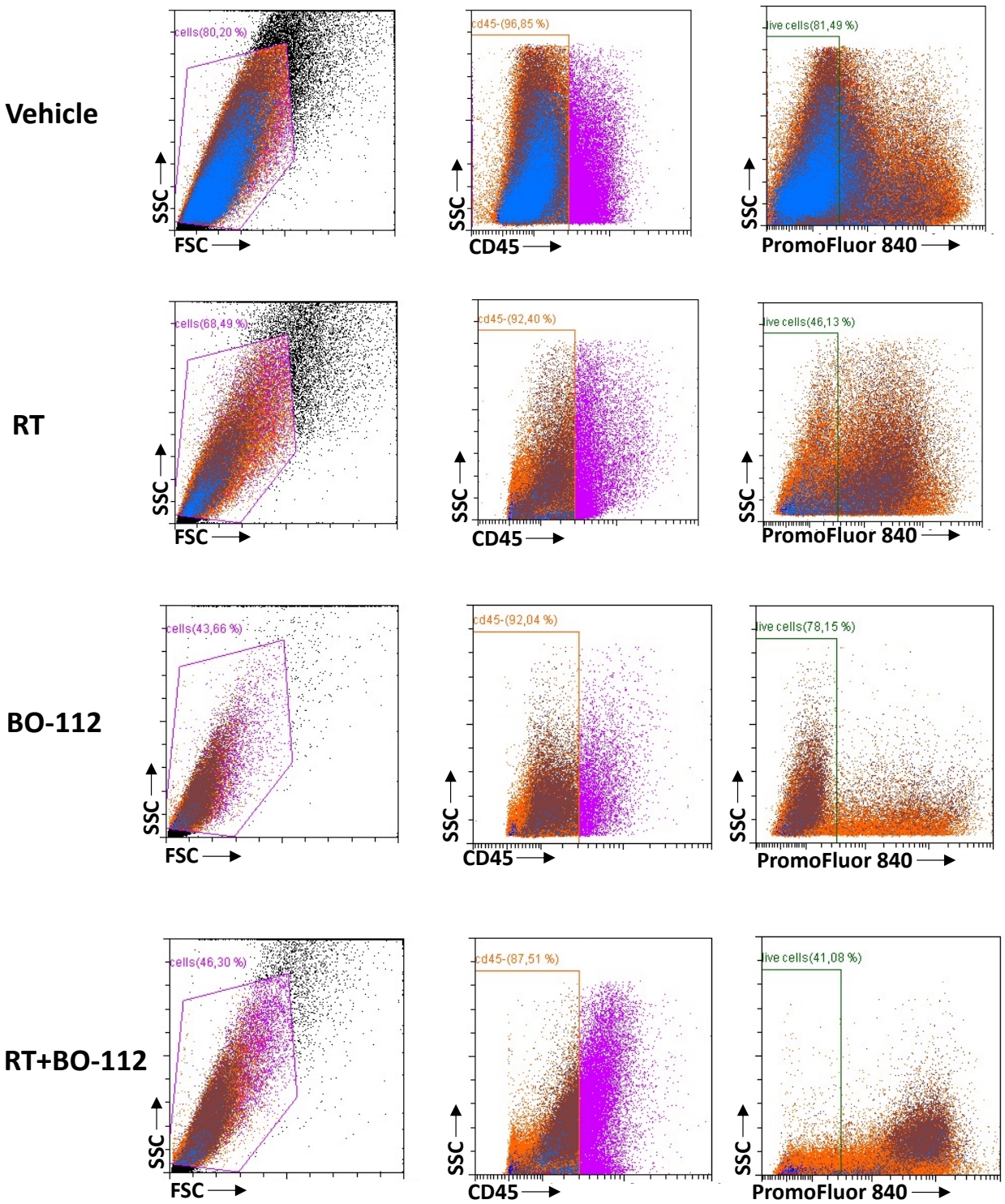

Supplemental Figure 7

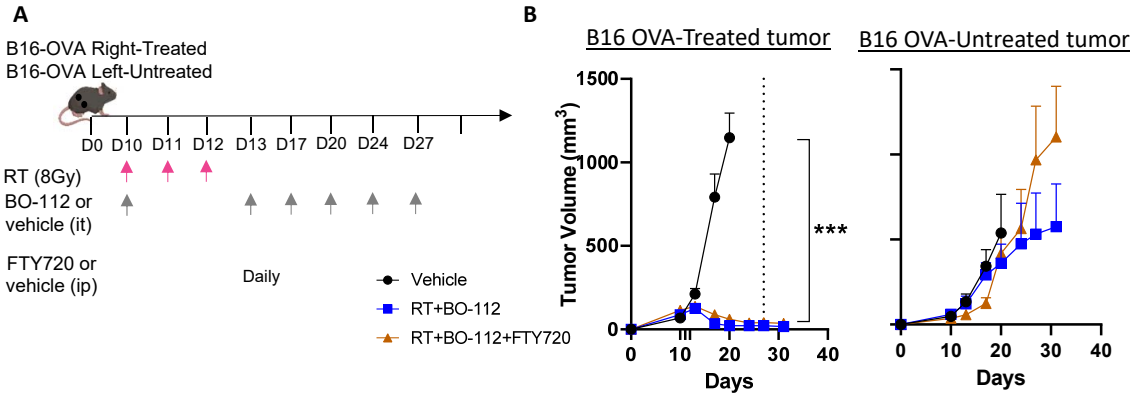

Supplemental Figure 8

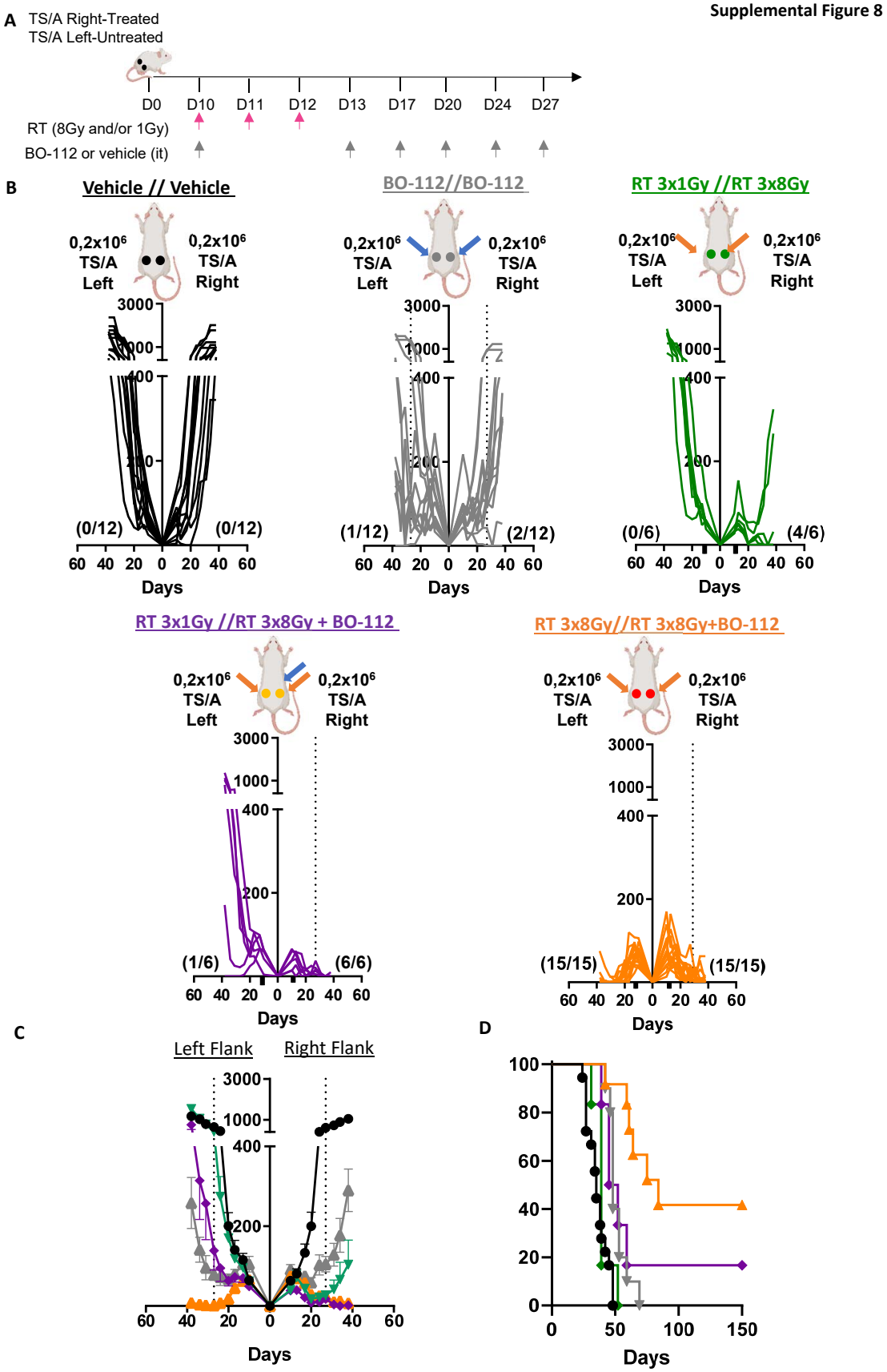

	Left flank					Right flank				
	Vehicle Vehicle	BO-112 BO-112	RT 3x1Gy RT 3x8Gy+BO-112	RT 3x8Gy RT 3x8Gy+BO-112	RT 3x1Gy RT 3x8Gy	Vehicle Vehicle	BO-112 BO-112	RT 3x1Gy RT 3x8Gy+BO-112	RT 3x8Gy RT 3x8Gy+BO-112	RT 3x1Gy RT 3x8Gy
Vehicle//Vehicle		***	**	***	*		***	***	***	***
BO-112//BO-112			***	*ns*	***			**	***	*ns*
RT 3x1Gy// RT 3x8Gy+BO-112				***	***				*ns*	*ns*
RT 3x8Gy// RT 3x8Gy+BO-112					***					*ns*
RT 3x1Gy// RT 3x8Gy										

SUPPLEMENTAL MATERIAL

Supplemental Figure 1. Gating strategy used for assessment of calreticulin surface exposure. (A) Representative gating strategy in single cell suspensions, depicting annexinV positive and calreticulin positive cells.

Supplemental Figure 2. Both BO-112 and irradiation induce features of immunogenic cell death. In experiments as schematized in figure 1B the concentrations of IFNß and ATP were assessed in the culture supernatants 24 and 48 hours after treatment (A and B). Results show means ± SEM (One-way ANOVA), n = 2–3 independent experiments, *$p < 0.05$, **$p < 0.01$***$p < 0.001$

Supplemental Figure 3. Local BO-112 synergizes with radiotherapy to control irradiated tumor lesions in the B16-OVA mouse model. (A) Scheme of 10-day tumor engraftment and subsequent treatments with hypofractionated radiotherapy and intratumoral injections of BO-112 in bilateral subcutaneous B16-OVA-derived tumors whose size was monitored. Radiotherapy and BO-112 were given to the same tumor lesions. (B) Means ± SEM and statistical comparisons. (C) Individual tumor sizes in the treated and distant untreated tumors are shown as indicated. (D) Kaplan Meier graph observed survival until 30 days. (E) Scheme of 10-day tumor engraftment and subsequent treatments with hypofractionated radiotherapy and intratumoral injections of BO-112 in bilateral subcutaneous B16-OVA in IFNAR KO mice whose size was monitored. m (F) Means ± SEM and statistical comparisons. Two-Way ANOVA test was used to assess significance; *$p < 0.05$, **$p < 0.01$, ***$p < 0.001$

Supplemental Figure 4 Dosimetry in mice bearing bilateral transplanted tumors. Representative dose distribution of focal irradiation in mice bearing two tumors subcutaneously engrafted in opposite flanks. (A) 3D-reconstruction of

the tumor-bearing mouse under general anesthesia with the irradiation beam represented as a white shadow. Isodose curves on a representative tumor-bearing mouse are shown in a CT-SCAN (axial, sagittal and coronal sections) with the ipsilateral (to be irradiated tumor in green) and the contralateral tumor out of the field in blue. Tumors are located in opposite sides of the mice to maximize distance and ensure that one of the lesions does not receive irradiation. (B) A dose volume histogram (DVH) represents in red line the treated tumor and in blue line the untreated tumor lesion. The inset summary table provides relative doses in cGy (mean, minimal and maximal values) for treated and untreated tumor lesions.

Supplemental Figure 5. Combination of systemic PD-1 and CTLA-4 blockade with dual intratumoral BO-112 plus radiotherapy enhances abscopal efficacy. (A) Scheme of treatments of, TS/A derived-tumor bearing mice. Mice received BO-112 and the corresponding intraperitoneal immunostimulatory monoclonal antibodies at 100 microgram doses after radiotherapy given on days 12, 15 and 18 for μ-CTLA-4 and on days 10, 13, 17, 20, 24, 27 for μ-PD-1 post-tumor cell inoculation. (B) Individual tumor growth (mm^3) is shown for each treatment groups showing treated tumors (upper panels) and untreated (lower panels) tumors. The dotted line indicates the last intratumoral injection of BO112. The numbers under each graph represent the fraction of mice in which complete tumor regression was attained. (C) The average tumor size (mean ± SEM) is followed for treated and untreated tumors. Data represent an experiment with six mice per group (mean ± SEM). Two-Way ANOVA was used to assess significance $*p < 0.05$, $**p < 0.01$, $***p < 0.001$.

Supplemental Figure 6. **Gating strategy used for tumor cell viability.** (A) Representative gating strategy from single cell suspensions, selecting CD45 negative and PromoFluor 840 negative to define live cells.

Supplemental Figure 7. T cell aggression from lymph nodes is required for irradiation and BO-112 mediated antitumor effects. (A) Scheme of 10-day tumor engraftment and subsequent treatments with hypofractionated radiotherapy, intratumoral injections of BO-112 and intraperitoneal injections of FTY720 to bilateral subcutaneous B16-OVA tumor-bearing mice whose tumor size was subsequently monitored. (B) Means ± SEM and statistical comparisons. Two-Way ANOVA test was used to assess significance; ***$p <$ 0.001

Supplemental Figure 8. Low dose radiotherapy does not synergize with intratumoral BO-112. (A) Schematic representation of treatment in groups of mice bearing bilateral TS/A-derived tumors in which one of the tumor lesions received radiotherapy and/or intratumoral BO-112, while the contralateral tumors remained untreated, received low dose radiotherapy (1Gy/3fx) or hypofractionated radiotherapy (8Gy/3fx. (B) Individual follow-up of bilateral tumor sizes in mice receiving the indicated treatments in their right or left concomitat tumors. (C) Mean ± SEM of tumors sizes in the groups of mice in B with statistical comparisons and (D) the survival Kaplan Meier curves observed. A two-Way ANOVA test was used to assess significance. Significant differences are displayed for comparisons with different groups (**$p < 0.01$, ***$p < 0.001$).